공학석사 학위논문

RC Column Retrofit with Ultra High Performance Concrete

초고성능 콘크리트를 이용한 기둥 보강 연구

2017 년 2 월

서울대학교 대학원

건축학과

구 인 영

RC Column Retrofit with

Ultra High Performance Concrete

지도 교수 홍 성 걸

이 논문을 공학석사 학위논문으로 제출함
2017 년 2 월

서울대학교 대학원
건축학과
구 인 영

구인영의 공학석사 학위논문을 인준함
2017 년 2 월

위 원 장 _____ (인)

부위원장 _____ (인)

위   원 _____ (인)

Abstract

RC Column Retrofit with Ultra High Performance Concrete

Koo, In Yeong

Department of Architecture and Architectural Engineering

College of Engineering

Seoul National University

Ultra high performance concrete is a material that can exert a compressive strength of 180 MPa or more and a tensile strength over 10 MPa. Recently, researches and applications of UHPC as a structural retrofit material for existing structural members are actively proceeding. This study deals with a column retrofit with UHPC jacket that can efficiently utilize strong compressive capacity of UHPC. The UHPC column retrofit method can allow jacket designed in less thickness than ordinary concrete jacketing. Also, it is expected to have superior strengthening performance compared to other column retrofitting methods. Furthermore excellent performances are expected in durability, fire resistance, and abrasion resistance.

The purpose of this study is to evaluate the strengtheningt performance of UHPC jackets. Considering the constructability for jacketing, any inserting additional flexural reinforcement or shear connectors were not considered and only pure jacketing performances were estimated. The main focus of this research was on the evaluation of strengthening performance for lateral load

resistance capacity among various performances required for seismic strengthening of the column. For this purpose, experimental research and a theoretical analysis on the failure mode were carried out.

In the experiment, UHPC jacket was found out to have excellent the strengthening performance in lateral load resistance. In the case of specimens with no additional stirrup reinforcement, the columns were destroyed by the massive diagonal cracks on the jacket and as the cracks increased, the performance of jacket has decreased very abruptly. It was confirmed that UHPC jacketing may cause additional unexpected failure due to additional shear force applied to adjacent beams or slabs. Therefore, proper measures should be taken for this kind of unexpected failure.

In theoretical failure mode analysis, three failure modes were considered . For each failure mode, corresponding failure curve was plotted against the axial load and lateral load. When the lateral load acts on the flexural member, the interface shear force is larger than that of the general RC composite section due to the characteristic of the section in which the UHPC having strong rigidity surrounds the inner column. When the interface shear strength is not sufficiently large, the composite column is prone to fail by diagonal tension cracks in jacket. Therefore, it is recommended to control the occurrence and opening of cracks in the jacket by inserting additional reinforcing bars or meshes in the jacket for better performance and further researches on this method and performance will be required.

Keywords : UHPC, retrofit, column, seismic
Student Number : 2015-21094

Contents

List of Tables

List of Figures

Chapter 1. Introduction

1.1 Backgrounds

Korea is located inside an earthquake plate and thus its earthquake shows a moderate seismic tendency. However, thesedays the occurrence frequency of the earthquake in Korea has been gradually increasing. Especially, in 2016, there occurred the largest earthquake in Gyung-Ju, since the observance of earthquake started in 1978. Its magnitude was estimated up to 5.8. As population and national infrastructures are concentrated in urban areas, in case of an earthquake, huge damage is expected and it is urgent to prepare for an earthquake. Meanwhile, the domestic seismic design criteria was first introduced in 1988, and most of the structures built before that do not satisfy the seismic design criteria. Structural members of these buildings are considered to have weak seismic performance due to the wide spacing of the stirrup reinforcements and use of $90°$ hooks.

There are three widely used techniques for retrofitting RC columns: Reinforced concrete jacketing, FRP wrapping, steel jacketing. Concrete jacketing method is most frequently used in field. It can increase overall structural capacities such as axial load capacity, shear strength, flexural strength and deformation capacity. However, it requires jacket thickness higher than 70-100mm, leading to decrease architectural area while increasing total mass of structure. On the other hand, FRP wrapping and steel jacketing have advantages over concrete jacketing method such as much less thickness,

lower weight and better constructability. However, strengthening performances are only limited to shear strength and deformation capacity. Axial load capacity can be increased by confinement effect, but is limited in extent. Besides, durability matters like fire or corrosion resistance should come into consideration when applying these methods.

Recently, a new retrofit technique using UHPFRC jacket to complement the weak points of existing method has been researched and applied to real structures. UHPFRC is an ultra-high performance fiber reinforced concrete of which compressive strength can reach over 180MPa and tensile strength over 10MPa by included fiber. This high strength can make it possible to exhibit higher strengthening effect than using normal concrete jacket. Also, due to high fluidity of UHPFRC, jacket thickness can reduce less than 30~50mm, thus, minimize the main disadvantage of normal concrete jacketing method. There are other advantages of UHPFRC retrofit such as high durability, good adjustability with various situations and that it can be combined optionally with other materials like wire mesh or textile mesh for better performances.

1.2 Scope and Objectives

The main goal of this research is to estimate strengthnening effect of UHPC jacket for a sqaure RC column. Especially, the lateral load bearing capacity of UHPC jacketed RC column is on the focus. The jacketing method is limited to discontinuous jacket for a high constructability. It means that the jacket is not physically connected to adjacent beam or stub, which would be very difficult to install within a thin thickness of the jacket.

The structural experiment was performed to compare the maximum lateral load before and after jacketing. The experiment was planned to focus on evaluating lateral load bearing capacity. Theoretical analysis was also conducted based on experimental results. Failure modes for a retrofitted column were defined and corresponding failure loads were estimated.

Column Jacketing

Beam overlay
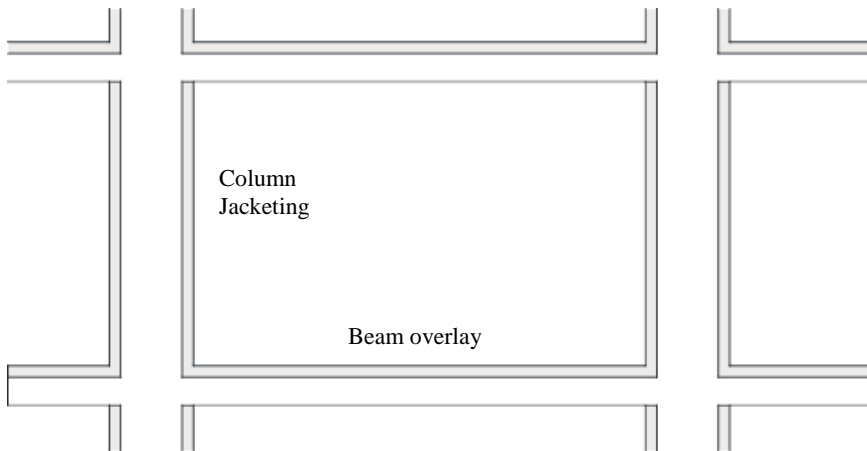
Fig. 1-1 Prototype of UHPC retrofit for an existing RC frame

Chapter 2. Literature Review

2.1 Ultra High Performance Concrete

There are several characteristics of UHPC which shows that it could be an appropriate material to be applied as a reparing substance.

• Very high mechanical strength: The very dense microstructure due to its very low water/binder ratio of only about 0.20 allow it to haver high compressive strength up to seven times more than normal concrete. Also, due to steel fibers inserted, it can have tensile strength up to 10MPa and exhibit ductile behavior.

• Extremely low permeability: The high density of the UHPC matrix brings extremely low permeability which mostly prevents the deleterious environmental influences such as water and chlorides. UHPC also shows high resistance of abrasion so that as a rehabilitation material, it can protect inner structures effectively from physical damages.

• High fluidity: The high liquidity of UHPC allows it to adjust various situations and circumstances. It can flow through relatively thin spaces so that when applied to existing structures as a jacketing method, it can minimize the required jacket thickness more than other materials. Also, when it is applied to deteriorated concrete structures, it can permeate damaged parts or cracks so that it can rehabilitate damages more efficiently.

2.2 Retrofitting RC column with concrete jacket

Beschi conducted two full-scale tests demonstrating the efficiency of the HPFRC jacketing technique. With the application of a high performance fiber reinforced concrete jacket, he showed that it was possible to increase the bearing capacity of the column and of the beam column joint, reaching also an adequate level of ductility. He concluded that the proposed technique resulted suitable for strengthening existing RC structures characterized by low concrete strength and low reinforcement ratios. In addition, the possibility of applying a thin concrete jacket did not substantially change the stiffness of structure, which might be relevant when the stiffness distribution of the original building should not be significantly modified. Finally, it was important to remark that the use of a self-compacting HPFRC jacket results in very smooth cast surfaces, allowing avoiding the use of finishing plaster layers, with an obvious advantage in terms of reduction geometry variations in the structure.

Meda conducted an experiment about strengthening of corroded RC columns with fiber reinforced concrete jacket. Reinforcement corrosion can induce severe damage in reinforced concrete (RC) columns leading to a relevant loss of bearing capacity. This condition can be even more critical in case of seismic events. The possibility of repairing and strengthening corrosion damaged columns with high performance fiber RC (HPFRC) jacketing was investigated. The main aim of the retrofit was, not only to restore the original bearing capacity, but also to increase the column durability. In order to investigate the effectiveness of the proposed technique, full-scale

tests on RC columns under cyclic loads was performed. Two columns were artificially corroded and one of them was repaired with a HPFRC jacket. This study concluded that The use of a high performance concrete layer can protect the core RC column and enhance its durability.

Zakaria studied aiming at investigating the effectiveness of strengthening the entire height of downscaled square RC columns by applying Forta Ferro Polypropylene Fibrous Ultra High Performance Self Compacting Concrete (Fibrous UHPSCC) as a jacketing material. He concluded that the self-compaction behavior of the Fibrous UHPSCC is very effective in casting the RC column jackets easily without manual compaction. The benefits of using self-compacting concrete is the fact that the jacketing thickness can be relatively thin and steel congestion which often causes segregation and honeycombing problems can be lessened. It is recommended to strengthen the four sides of square RC columns using the Fibrous UHPSCC as a jacketing material, as it is a high compressive strength material and reinforced by fibers which enhanced the ductility and reduced the jacketing thickness.

2.3 Interface shear strength model

In Eurocode 2, the interface shear strength between two concrete layers cast at different times is proposed as a summation of three main elements given as:

$$\tau_{if,allow} = c \cdot f_{ctd} + \mu\sigma_n + \rho f_{yd}\left(\mu\sin\alpha + \cos\alpha\right) \le 0.5\nu f_{cd} \quad (1)$$

In this equation, $c \cdot f_{ctd}$ refers to the concrete cohesion strength resulting from concrete chemical adhesion in the interface layer, where c is the cohesion coefficient and f_{ctd} is the concrete tensile strength of the concrete topping layer. $\mu\sigma_n$ is a frictional stress factor resulting from the friction coefficient at the interface, μ and σ_n which is the normal stress. $\rho f_{yd}\left(\mu\sin\alpha + \cos\alpha\right)$ is a clamping stress component resulting from the steel reinforcements crossing the interface, in which ρ is the reinforcement ratio, f_{yd} is the design yield stress of the reinforcement and α is the angle between the steel reinforcement and the plane and ν is strength reduction function. Design expression in Eurocode 2 is based on qualitative observation of the surface textures that range from very smooth to very rough. The recommendation of roughness height for rough surface should be at least 3 mm and for indented or very rough surface at least 5 mm. The value of the friction coefficient has a variation from 0.50 – 0.90, while the cohesion coefficient ranged from 0.025 – 0.50. These valures are corresponding to the surface profile from very smooth to very rough.

CEB-FIB Model Code 2010 quantifies the surface roughness using the average roughness, R_a which is determined as the mean value of texture

height along a certain length, l_m. The surface texture is measured and categorized from very smooth to very rough. Very smooth is where the surface is cast against steel formwork, thus R_a is not measurable. Meanwhile, smooth surface is untreated and cast against wooden formwork where R_a is taken as less than 1.5 mm, and rough surface is roughened by sand blasting where R_a is more than 1.5 mm. For very rough surface, the surface is roughened using high pressure water jet where the indented has an R_a of more than 3 mm. The friction coefficient ranged from 0.50 – 1.40, and the concrete adhesion is categorized into rough and very rough surface with the mean shear resistance ranged from 1.5 – 3.5 N/mm2. The interface shear strength equation is given as:

$$\tau = \tau_c + \mu\left(\sigma_n + \kappa \cdot \rho \cdot f_y\right) \tag{2}$$

where, κ is the interaction "effectiveness" factor and τ_c is the adhesion or interlocking mechanism. The term $\mu\left(\sigma_n + \kappa \cdot \rho \cdot f_y\right)$ is contributed from friction and dowel action. The assessment on the strong adhesive bonding is when the adhesive bonding and interlocking are the main contributing mechanisms to the interface shear strength, while the weak adhesive bonding is when friction and dowel action are the main contributing mechanisms to the interface shear strength.

2.4 Direct shear strength model of UHPFRC

The direct shear strength of UHPFRC can be presented in a similar composition which is a combination of three components: cohesion, friction and dowel action. However, in UHPFRC, the contribution of steel fibers should be taken into account in frictional factor. Lee at al suggested the frictional shear strength of UHPFRC given as equation (3) based on the experimental analysis and plasticity theory. However, $\mu f_{ctd} A_{cc}/K$ was added to the basic frictional shear strength equation of normal concrete. It was assumed that the tensile strength by steel fiber is applied as an average normal confinement force to cracking plane. The upper limit of shear friction strength was defined as an upper limit of shear strength suggested by K-UHPC structure design guidelines issued by Korea Concrete Institute, assuming that it is a strength by compressive strut rupture of UHPC. For a monolitic structure, cohesion coefficient c of UHPC is defined to be 2.0 MPa and friction coefficient μ to be 1.4.

$$V_{cwd} = \tau_c A_{cc} + \mu\left(\sigma_n + f_{u,ctd}/K\right)A_{cc} + f_{yd}\left(\mu\sin\alpha + \cos\alpha\right)A_w$$
$$\leq 0.84 f_{u,cd}^{2/3} A_{cc} \tag{3}$$

Chapter 3. Experimental Research

3.1 Experiment program

3.1.1 Introduction

As indicated in chapter 2.2, previous experiments about column strengthening with UHPC or HRC are only dealing with single curvature columns. .In single curvature column, required shear capaticy is usually lower than flexural capacity, because a/d ratio of single-curvature column is twice as large as that of double-curvature column. Hence, previous researches were focusing on flexural strengtheing effect of UHPC jacket. However, in real building, usually, columns have double curvature when applied lateral load. And for unseismic designed columns are normally more vulernable to shear than flexure.

This experiment focuses on shear strengthening performance of UHPC jacket. For this purpose, column specimens were planed in double curvature and designed to be governed by shear capacity, not by flexural capacity when applied lateral load. There are several factors to be estimated in seismic retrofit experiments such as lateral load resistance capacity, ductility, stiffness, energy dissipation, etc. Among these factors, this research and the experiments mainly concentrated to estimate strenghenging lateral load resistance performace of UHPC jacket. Jacket thickess and additional stirrup reinforcement insert were planned as variables.

3.1.2 Geometry & material detail of retrofitting target
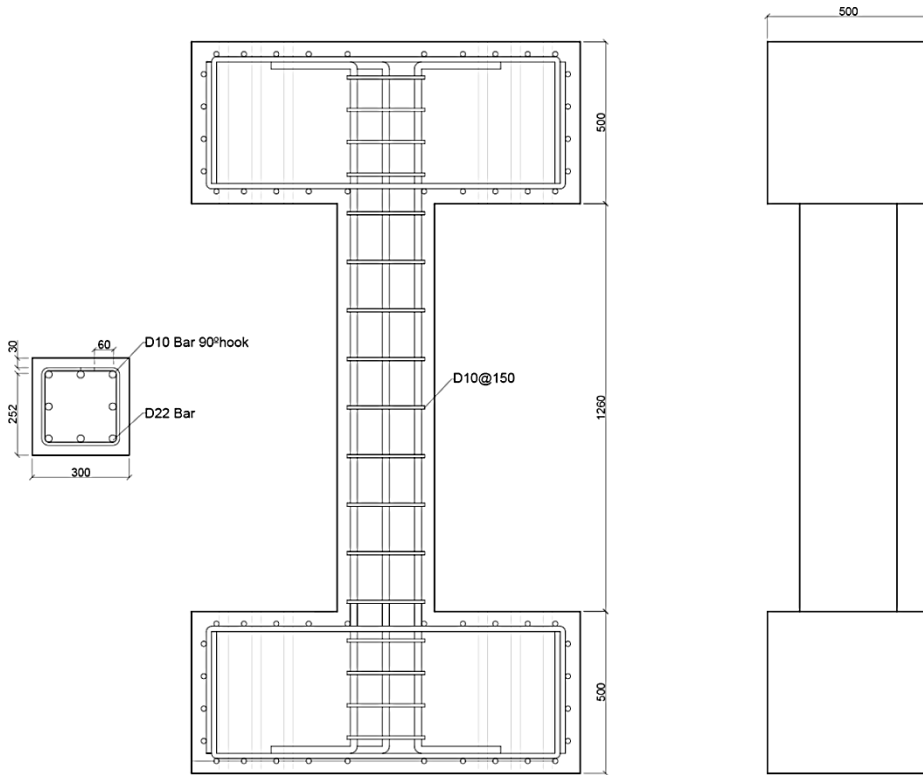
Fig. 3-1 Geometry of RC column

Four identical RC column specimens were manufactured in half scale. The dimensions adopted for the column cross section and height were 300×300mm and 1260mm, respectively. The corresponding span to depth ratio is 4.15. The longitudinal reinforcement consisted of eight 22mm diameter bars and corresponding reinforcement ratio is 3.44%. These relatively small span to depth ratio and large reinforcement ratio were intended to make a shear failure mode both in before and after retrofitting, in order to make it clear to define shear strength of specimens. The transverse reinforcement comprised of 10mm diameter stirrups with 150mm spacing.

The column has 500×500mm foundations at both upper and lower stubs to have double curvature experiment. Detail geometres and material properites of the RC column are described in Fig. 3-1 and Table 3-1.

Table 3-1 Properties of retrofitting target

Column geometry	section	300mm × 300mm
	Height, h	1260mm
Longitudinal reinforcement		8 × HD22
Transverse reinforcement		HD10@150mm
Nominal strength	Concrete, f_c'	24 MPa
	Reinforcement, f_y	400 MPa (SS400)

3.1.3 Nominal strength of retrofitting target column

a) Moment capacity

The nominal moment capacity of the target column can be estimated using strain compatibility solution. This process starts with assuming linear strain distribution among the whole section and setting the value of the strain of extreme compressive fiber, $\varepsilon_{cu} = 0.003$. With a stress-strain relationship of materials, the stress distribution and corresponding net normal force and moment can be calculated. The process is briefly described in Fig. 3-2. The iteration of this process while varying the neutral axis location, gives the P-M interation diagram. Fig. 3-3 shows the resultant P-M interation diagram for this RC section. Herein, any strength reduction factor was not considered.

(a) Strain distribution

(b) Force distribution
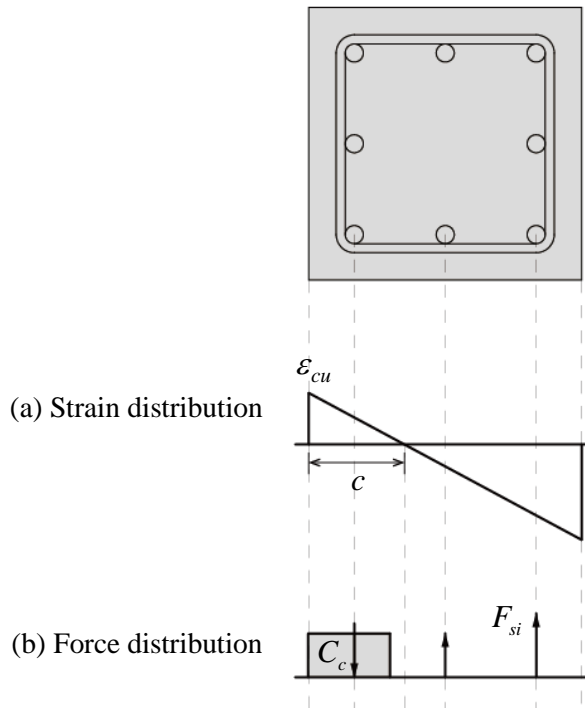
Fig. 3-2 Strain compatibility solution

Considering that the column is designed to have double curvature in bending, the maximum bending moment, M shoud satisfy equation **(4)**

$$M = VL/2 \qquad \qquad (4)$$

where,

V = lateral load applied to column

L = length of the column

From the equation (22), the P-M interaction diagram of Fig. 3-3 can be transformed to P-V interaction diagram, as shown in solid line of Fig. 3-4.
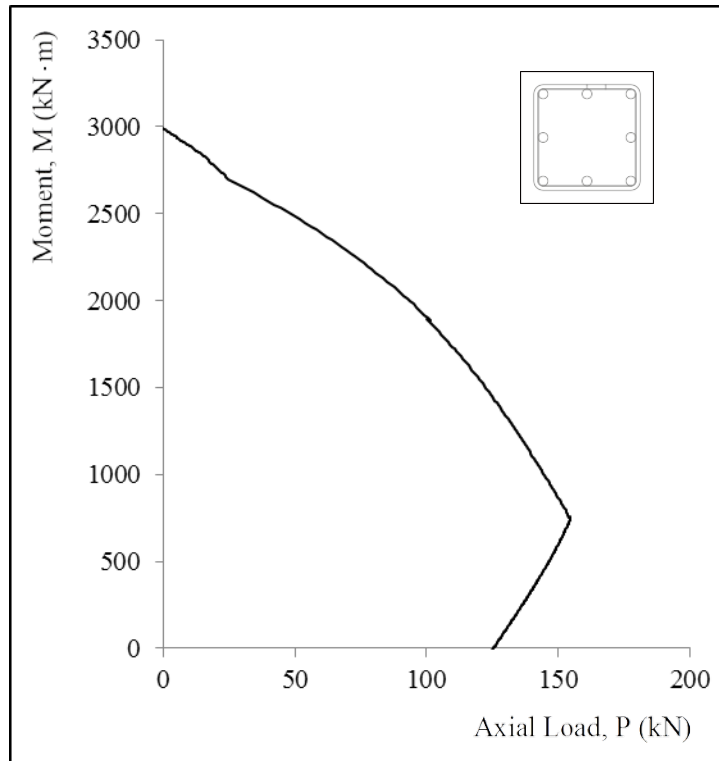
Fig. 3-3 P-M interaction diagram for the target RC column

b) Shear capacity

The shear strength, V_n of the target column can be calculated from the following equations **(5)** -**(7)** in ACI 318-11.

$$V_n = V_c + V_s \tag{5}$$

$$V_c = 0.17 \left(1 + \frac{P}{14 A_g} \right) \sqrt{f_c'} \, b_w d \tag{6}$$

$$V_s = \frac{A_v f_{yt} d}{s} \tag{7}$$

where,

f_{yt} = nominal strength of stirrup reinforcement (MPa)

s = stirrup spacing (mm)

The resultant shear strengh with respect to axial load, P is plotted with dotted line in Fig. 3-4. This graph shows that the column would be governed by shear failure at lower axial load and by flexural failure at higher axial load. The axial load in this experiment was $0.3 A_g f_c'$ so that the target column would fail in flexural failure.
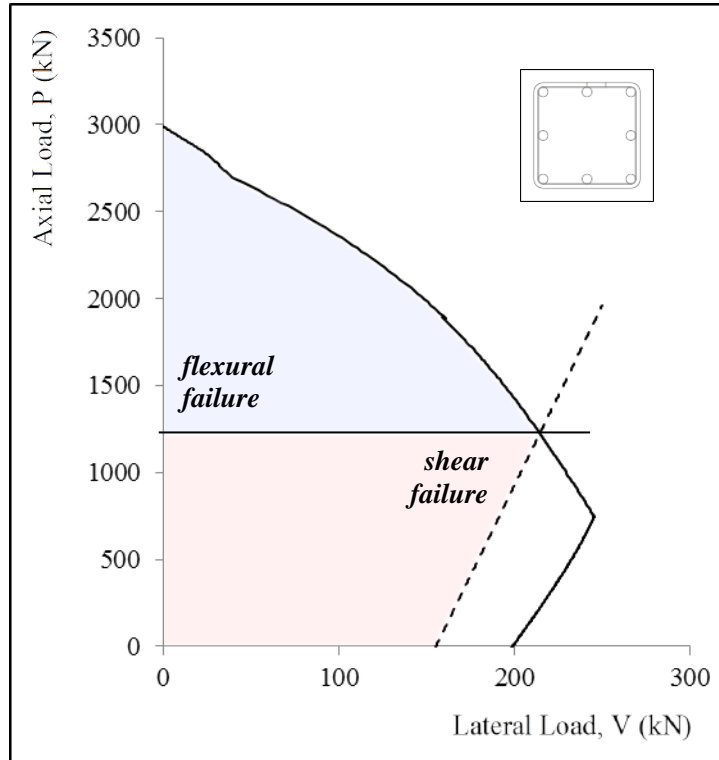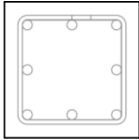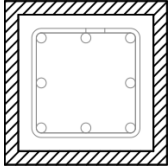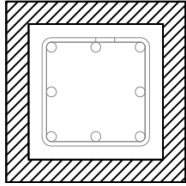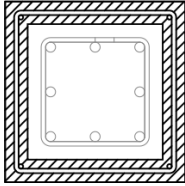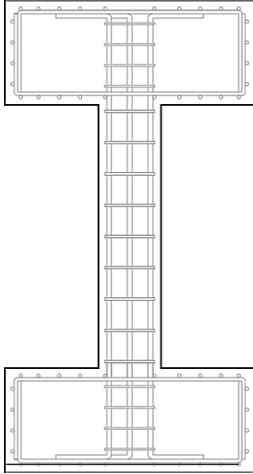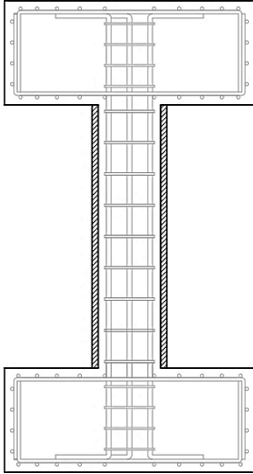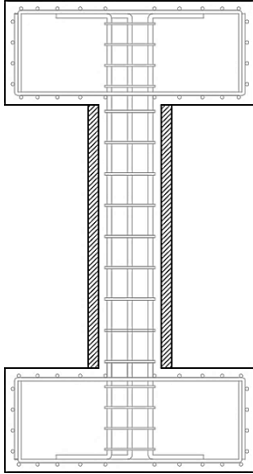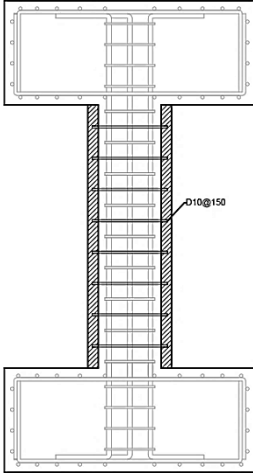
Fig. 3-4 P-V interaction diagram for the target RC column

3.1.4 Test variable

Four RC columns were retrofitted in different ways. The jacket thickness was chosen as a main variable. R-0 remained unretrofitted as a reference specimen. R-30 and R-50 were retrofitted by 30mm and 50mm UHPC jacket, respectively. 30mm was chosen as it is 10% of the column width. 50mm was chosen, because this thickess was thought as the minimum thickness that could afford additional reinforcement in jackets. The details of the three specimens are summarized in Table 3-2.

Table 3-2 Test variables and detail

	R-0	R-30	R-50	R-50S
Retrofit Method	Reference	30mm jacket (10% thinkness)	50mm jacket (16.7% thickness)	50mm jacket + additianl striups
Section				
Elevation				

3.1.5 Manufacturing process

The manufacturing processes of the test specimens are shown in Fig. 3-7. First of all, three identical RC columns were manufactured (Fig. 3-7 (a)-(c)). After concrete curing had finished, the surface of the column was sandblasted by 100MPa air pressure so that the surface roughness could reach about 3-4mm (Fig. 3-7 (e)). This surface roughening technique was already demonstrated effective by Martinola et al (2010). Fig. 3-5 shows the image of the column surface before and after sandblasting.

Then, the jacketing forms were installed for R-30 and R-50. For the convenience in UHPC pouring, the formwork were made lied down(Fig. 3-7 (f)). UHPC was mixed on the place and poured onto core column (Fig. 3-7 (g)). Fig. 3-7 shows that the slump test result of the UHPC was about 600mm, which shows high fluidity of the UHPC. After pouring, UHPC was cured in hot steams about 90℃ for 72 hours(Fig. 3-7 (h)).

Fig. 3-5 Surface before/after sandblast   **Fig. 3-6 UHPC slump test**
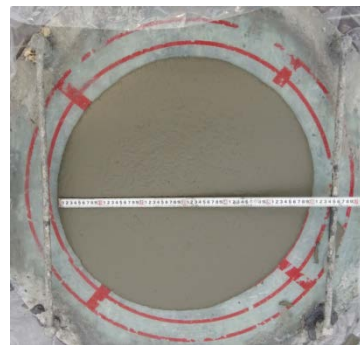
(a) Arrange reinforment bars

(b) Column formwork

(c) Concrete placing

(d) Disassemble formwork

(e) sandblasting

(f) jacketing formwork

(g) placing UHPC

(h) steam curing

Fig. 3-7 Manufacturing process of test specimens

3.1.6 Material property test results

The mixture portion of concrete with nominal compressive strength of 24MPa is shown inTable 3-3. Concrete standard specimens of 10cm×20cm size were casted according to KS F 2403 and 3 specimens were tested following with KS F 2405. The test results are shown in **Fig. 3-8** (a). Actual compressive strength of concrete came out to be 29.1MPa.

In the case of reinforcement used in this research, direct tension test results and material properties are listed inTable 3-4. D22 acting as main longitudinal reinforcement in RC columns showed 490MPa yield strength. D10 used as a stirrup reinforcement showed about 465MPa yield strength.

Table 3-3 Mixture portion of concrete

Nominal Strength (MPa)	W/C (%)	S/a (%)	Unit weight(kgf/m^3)				
			Cement	Water	Sand	Grave	Admixture
24	48	47.5	344	165	860	968	1.72

Table 3-4 Material properties of reinforcement

Diameter	Steel grade	f_{sy} (MPa)	f_{su} (MPa)	E_s (GPa)
D22	SD400	490	628	187
D10	SD400	465	628	187

(a)   (b)
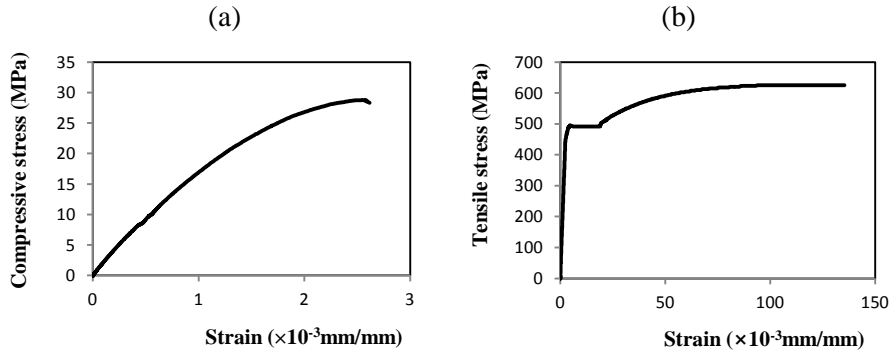
Fig. 3-8 Material properties of RC columns and additional reinforcements
a) Compressive stress-strain curve of concrete, b) Tensile stress-strain curve of
SD400 D22

The mixture portion of UHPC is specified in Table 3-5. The steel fiber used was only 13mm, which is a bit short, in order to prevent unexpected defect in UHPC pouring. The characteristic tensile strength of the fiber is 2500MPa according to manufacturer.

Compression test for UHPC was carried out in the same way for normal concrete. Its compressive strength came out to be 144MPa and maximum strain was about 0.004. The tensile strength was estimated to be 6.4MPa and tensile cracking strength was 4.9MPa.

Table 3-5 UHPC mixing portion

Nominal Strength (MPa)	W/B (%)	Mass proportion					
		Cement	Silica fume	Sand	Filling powder	Super-plasticizer	Steel fiber
180	20	1	0.25	1.1	0.3	0.018	1.5%

(a)　　　　　　　　　　　　　　　　(b)
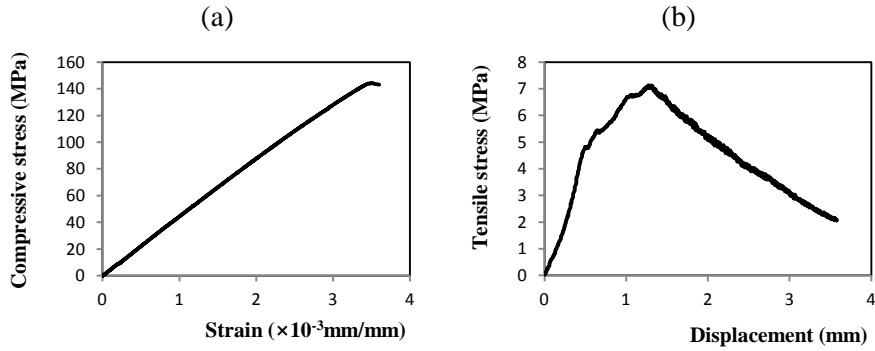
Fig. 3-9 UHPC material test results:
a) Compressive stress-strain curve, b) Tensile stress-displacement curve.

3.1.7 Test set-up and procedure

The four tests were conducted in the same set-up as presented in Fig. 3-11. Initial constant axial load of $P = 0.3 f_c' A_g$ was applied to column by two 100ton oil jacks and then, displacement controlled horizontal cyclic load V was applied by a 200ton actuator. The amplitude of imposed displacement of the first cycle was 3mm and increased by 3mm for every additional cycle up to 15mm, and thereafter increased by 6mm.
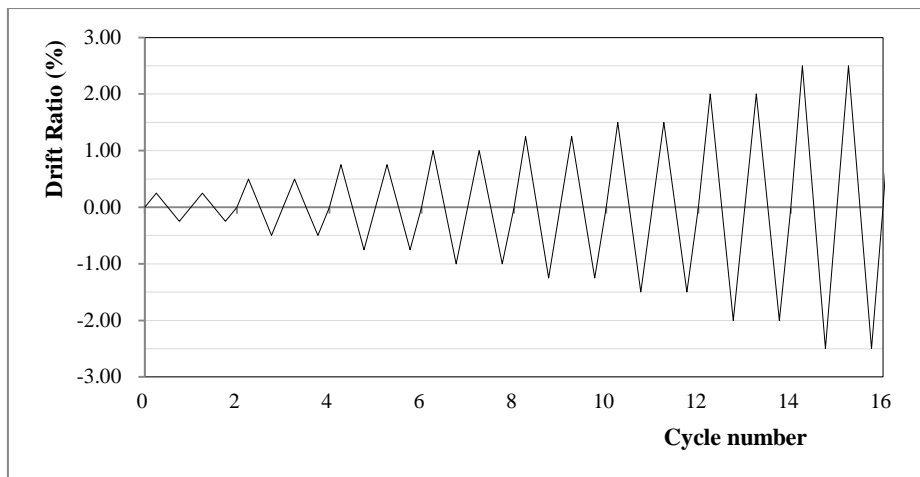
Fig. 3-10 Lateral loading protocol
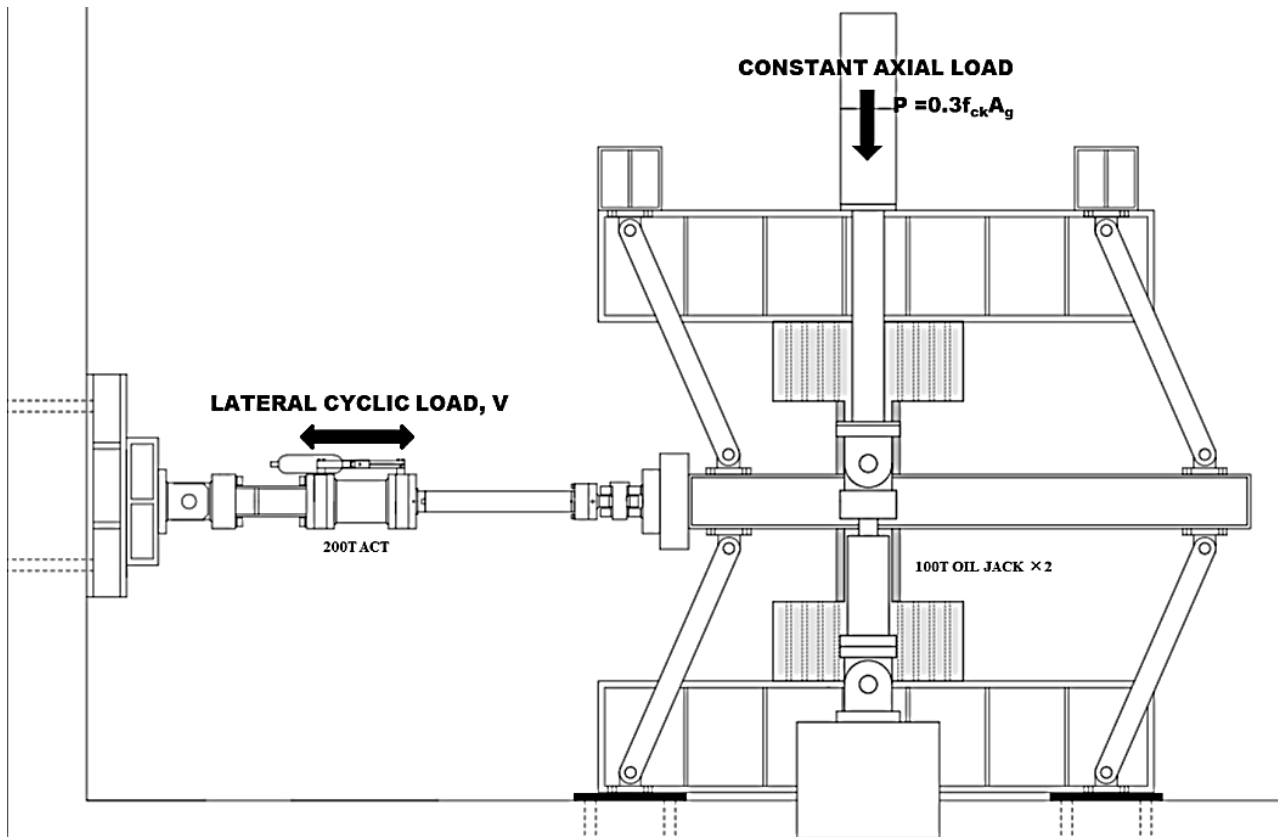
Fig. 3-11 Test set-up
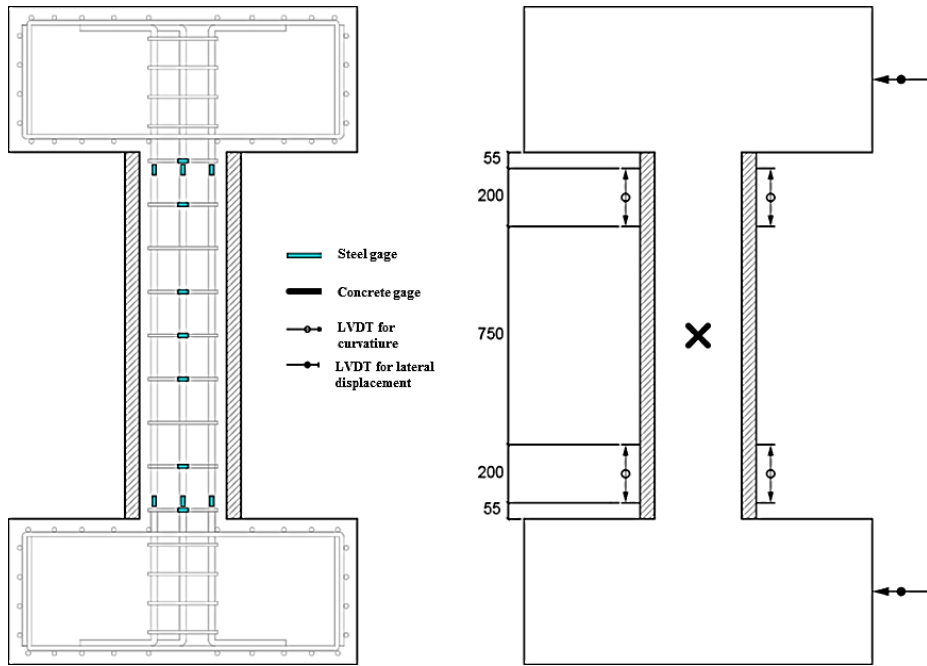
Fig. 3-12 Measurement set-up

Steel gauges were attached to the main longitudinal bars at both ends of the columns to measure the flexural curvature and yield point of the members. Steel gauges for stirrup bars were attached at the points where shear failure is expected. The shear deformation of the center part of the column was measured by attaching the concrete gauge in X shape. LVDT was installed in order to measure the flexural curvature of the end portion of the member where maximum flexural deformation is expected.

3.2 Test results

3.2.1 Reference RC column

The crack patterns of the unretrofitted reference specimen R-0 during and after test are as shown in Fig. 3-13. The initial cracks occurred around the end of the column as flexural cracks at 0.46% drift ratio. These cracks spread as flexural - shear cracks until 0.92%. However, when the displacement reached 1.16%, vertical cracks occurred rather than flexural - shear cracks, which were dominant until the previous stage. Afterwards, the strength had dropped abruptly. The vertical cracks almost coincide with the position and direction of the longitudinal reinforcements. Therefore, it can be seen that the failure mode was a bond failure due to the separation between the rebars and concrete. This is not the originally intended shear failure mode. It is inferred that due to the excessive amount of longitudinal rebars in small cross section had led to this unexpected bond failure. Also, tight loading cycles might have influenced on the result.

During the test, any rebars didn't reach the yield point. The maximum lateral load came out to be 210.4 kN and the maximum displacement was 1.16%. The resultant load-displacement curve is shown in Fig. 3-16

+0.69% drift

+1.16% drift

Final crack

E   S   W   N
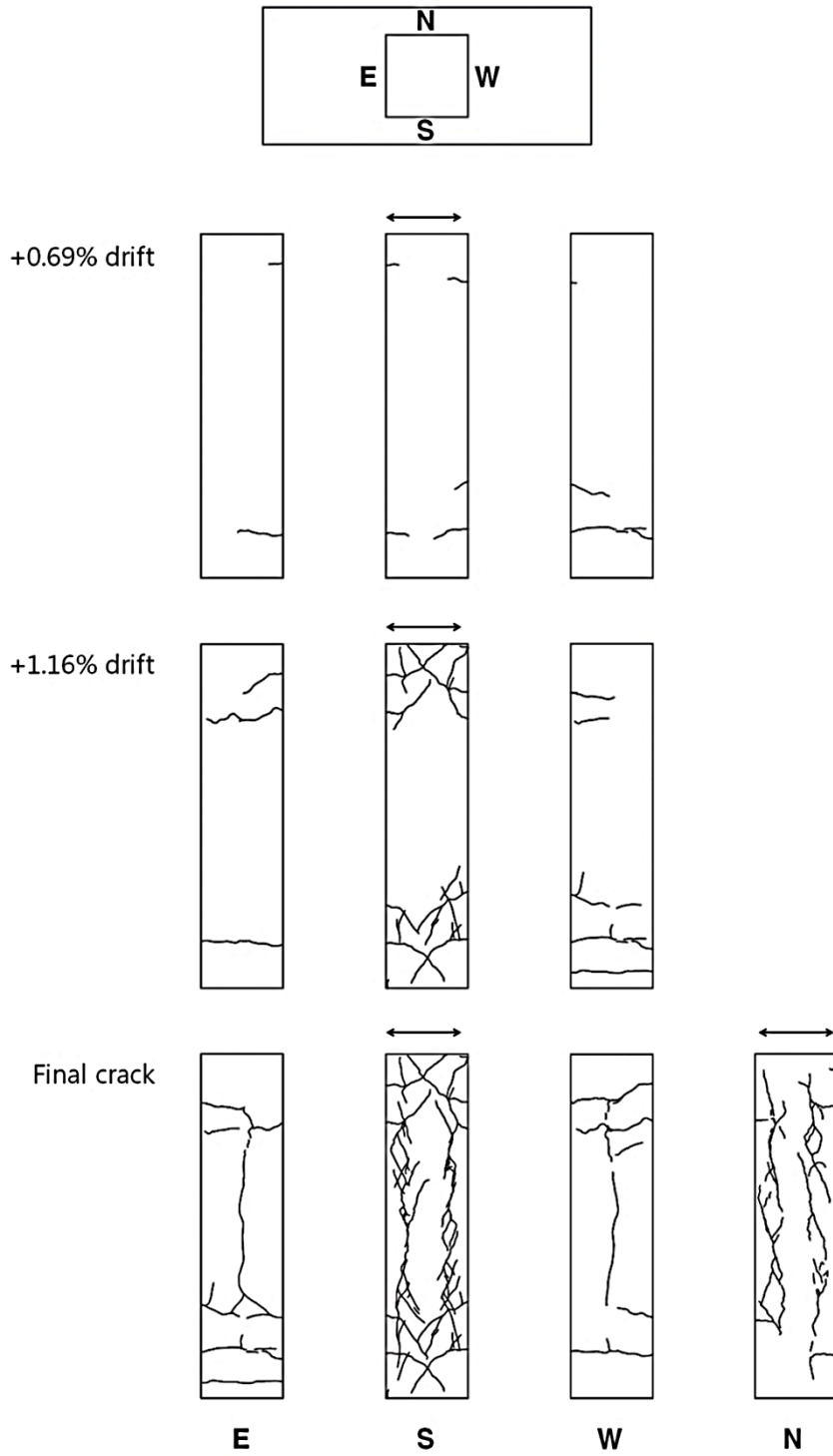
Fig. 3-13 Crack pattern (R-0)

26

3.2.2 RC column retrofitted by 30mm jacket (R-30)

The crack patterns of the R3 specimen reinforced with UHPC of 30mm is described in Fig. 3-14. Owing to the crack control capability of the steel fiber, any cracks in the column surface did not occur until the drift ratio reaches 0.90%, except for the separation between UHPC jacket and end stubs. When the displacement increased to 1.16%, there occured a large diagonal crack starting at column center. The strength was not immediately reduced right after the occurance of the cracks. However, as following load was applied, the diagonal cracks were spread over while other small cracks occurred simultaneously. As the massive crack reaches around the pull-out length of the steel fiber, the UHPC jacket does not function and the strength decreased drastically.

It was found that some of the longitudinal reinforcements had yielded around the maximum strength, but the diagonal cracks occurred almost at the same time so that it did not lead to the flexural yielding of the entire members. The maximum strength came out to be 359.8kN and the maximum displacement was 1.65%.

+0.69% drift

+1.16% drift

Final crack

E   S   W   N
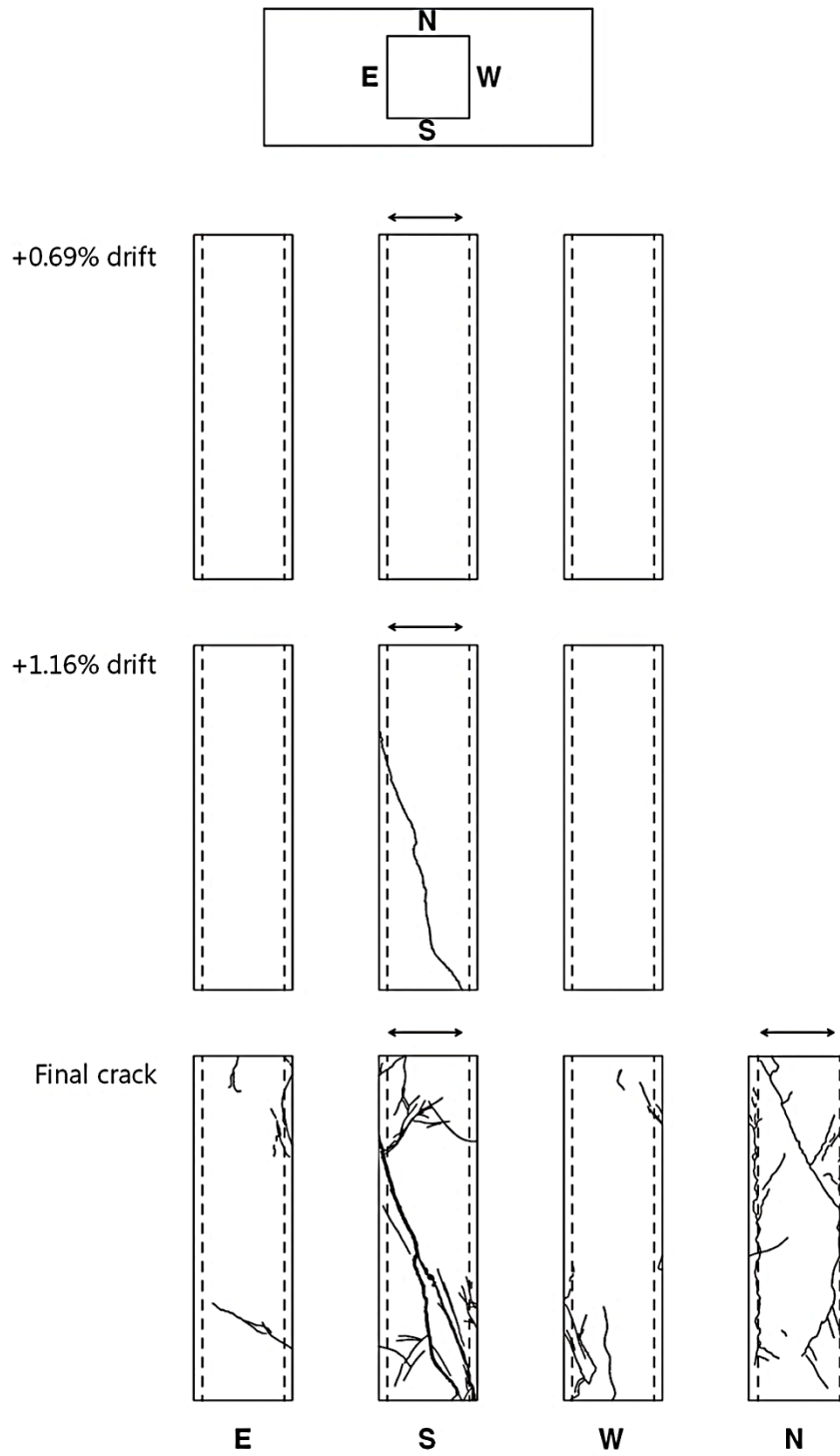
Fig. 3-14 Crack pattern (R-30)

3.2.3 RC column retrofitted by 50mm jacket (R-50)

For R-50 specimens retrofitted with 50mm UHPC jacket, cracks patterns and the failure mode appeared similar to those of R-30. At the drift ratio of 1.78%, some vertical cracks occurred in the compression zone. Thereafter, when the drift increased up to 2.20%, large diagonal cracks occurred at the upper part of the column. In contrast to R-30, diagonal cracks occured in both positive and negative directions. As the cracks of the diagonal cracks gradually spread, the steel fibers were observed to be pulled out or cut off from the UHPC matrices. It resulted in a sudden drop in lateral load capacity. It seems that when massive diagonal cracks opened, the UHPC jacket and the core column did not act as a unified section any more.

It was found that the longitudinal reinforcements yielded at 1.09% of drift ratio before the initial cracks occurred, and it was confirmed that the entire member showed yielding behavior from the load - displacement curve as shown in Fig. 3-18. The maximum lateral strength came out to be 478.9kN and the maximum displacement was 2.72%.
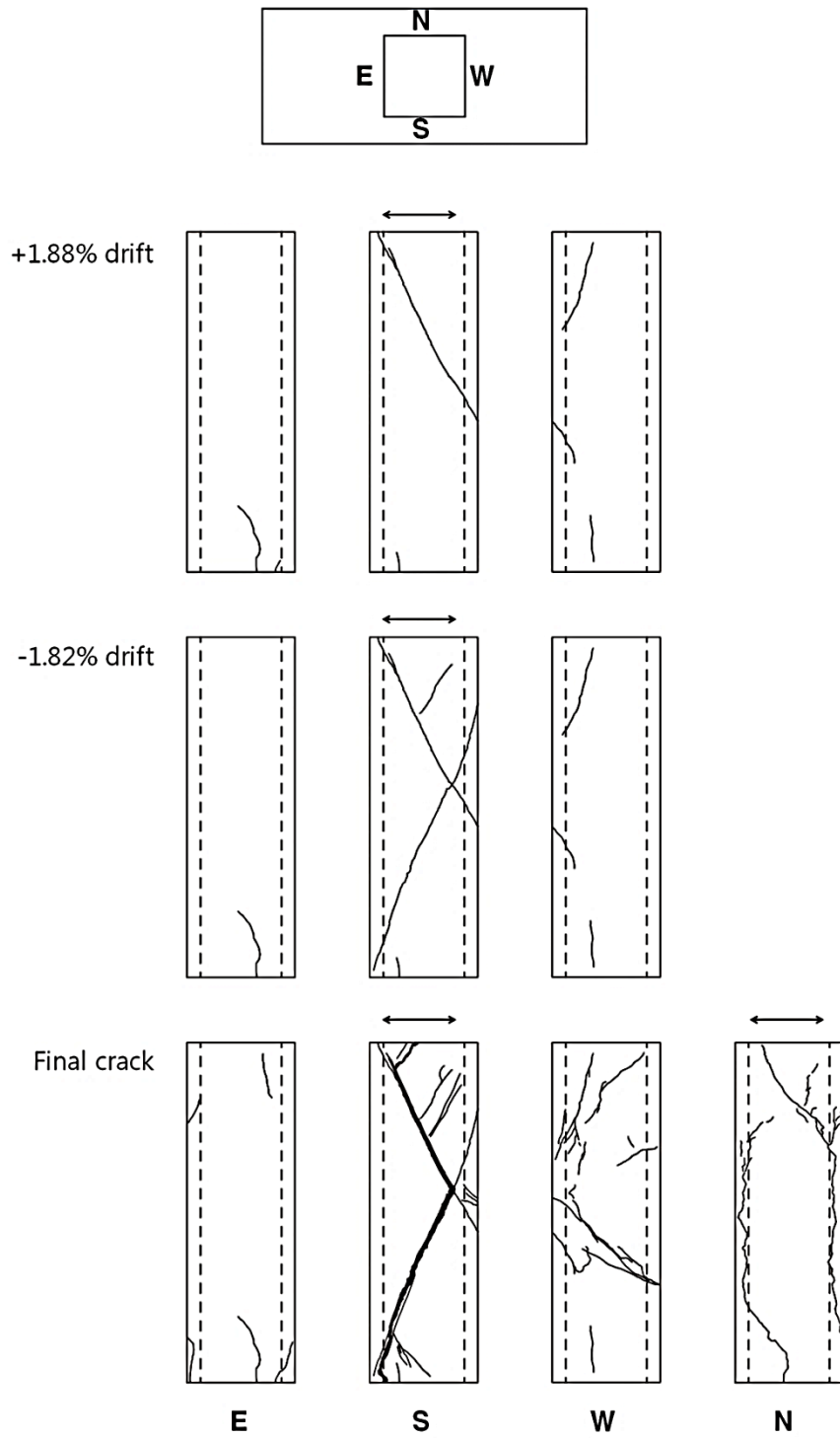
Fig. 3-15 Crack pattern (R-50)
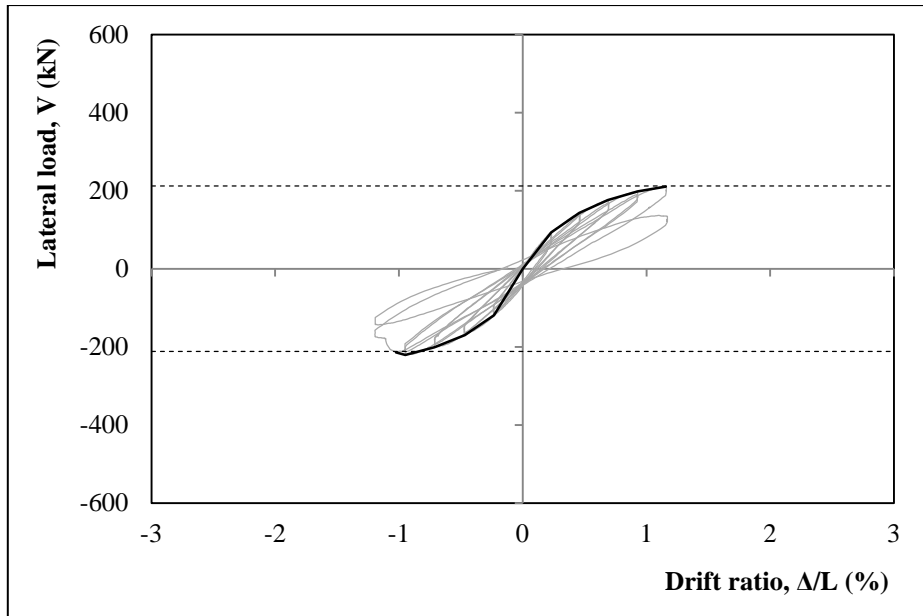
Fig. 3-16 Load-displacement curve (R-0)
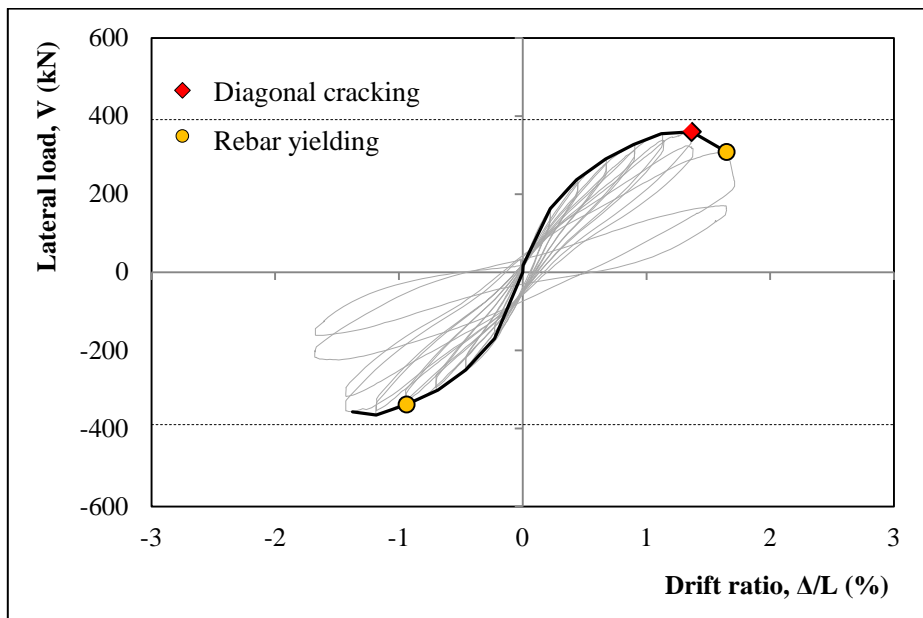
Fig. 3-17 Load-displacement curve (R-30)
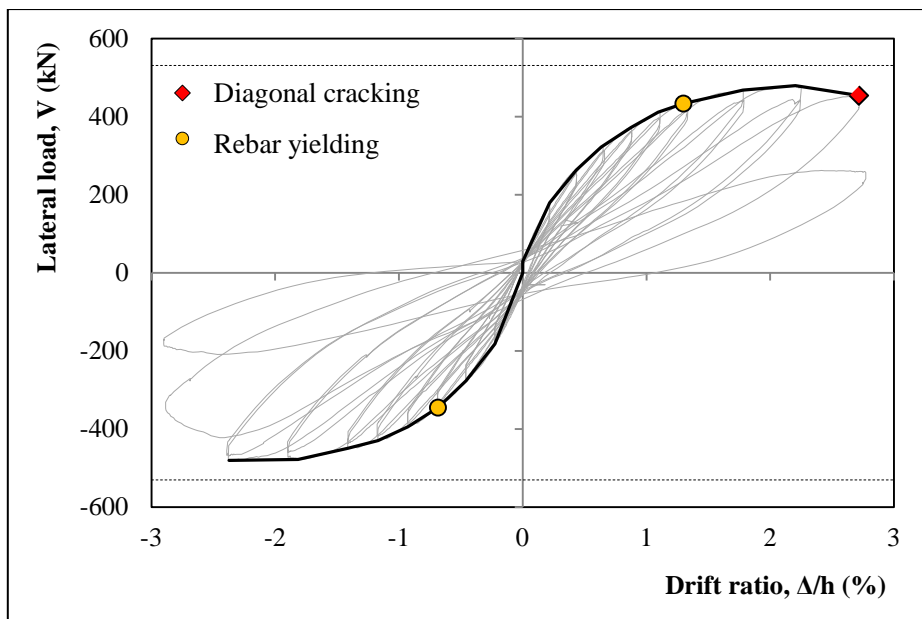
Fig. 3-18 Load-displacement curve (R-50)

Fig. 3-19 Crack opening process

Fig. 3-20 extended image of diagonal crack

3.2.4 Strengthening effect of UHPC jacket

Compared with the R-0 specimen, the maximum load capacities of R-30 and R-50 increased about 71% and 128%, respectively. The maximum strain increased about 42% and 134%, respectively. Considering that the column area increased 44% and 78%, the increase in strength was almost proportional to the increase in area. However, the maximum displacement of R-50 was superior to that of R-30. This is because in R-50, the rebars has reached the yield points and R-30 has been fractured before yielding.
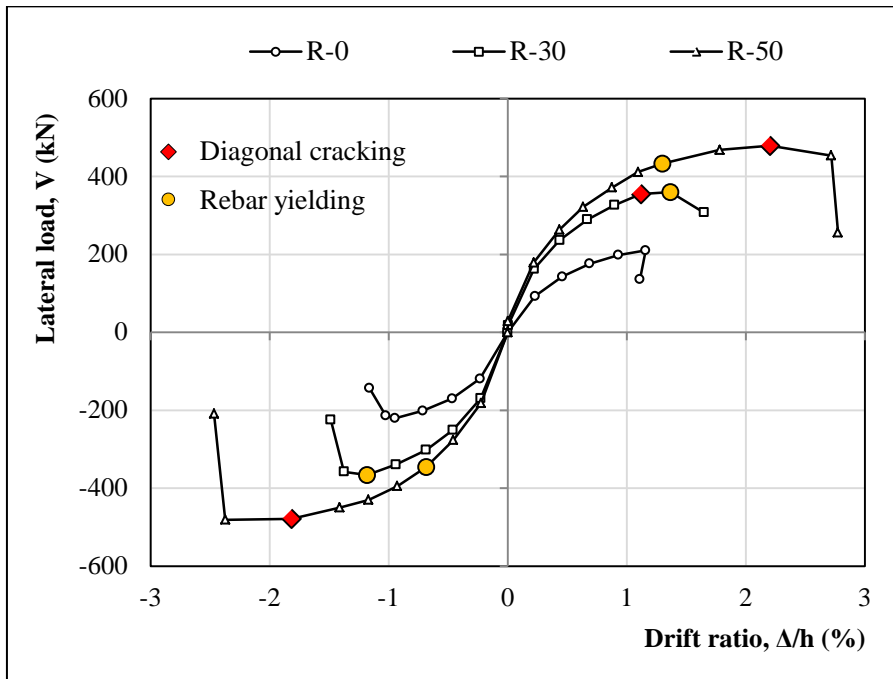
Fig. 3-21 Load-drift curve envelop

For each cycle, the point corresponding to 75% of the maximum value / additional force maximum strength is connected, and the stiffness is calculated from the drift by the slope, and the result is shown in Fig. 3-22.

The initial stiffness of unreinforced specimen R0 was 35.6kN, R3 was 68.0 kN / mm, and R5 was 76.2 kN / mm. It was confirmed that the stiffness increased by 91% and 114%, respectively. The decrease of the stiffness due to the displacement was linearly decreased in the R0 case, but in the case of the reinforced specimen, the decrease width was relatively large at the initial stage and then decreased linearly thereafter. This is due to the fact that unlike R0, the reinforced specimens show prominent lifting at the joints. After the initial rapid decline, stiffness reduction was observed to be similar to R0. At this time, the stiffness of R3 and R5 increased by 69% and 100%, respectively.
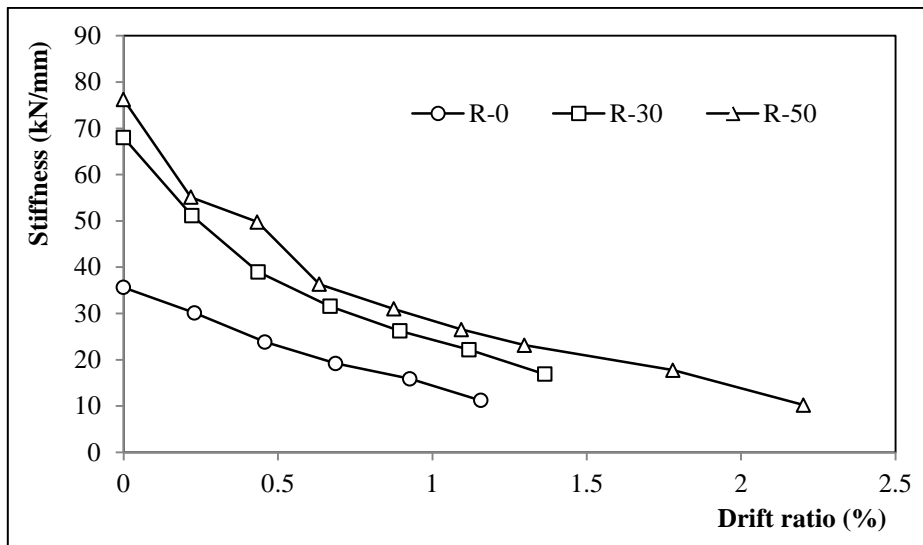
Fig. 3-22 Stiffness against displacement envelops

Table 3-6 Experiment result summary

	R0	R3	R5
Failure mode	bond	Diagonal tenile failure	Diagonal tenile failure
Retrofit method	-	30mm UHPC	50mm UHPC
Jacket thickness	-	10%	16.7%
Area increase	-	44%	77%
Max. strength	210.4 kN	359.8 kN	478.9 kN
Max. drift ratio	1.16 %	1.65 %	2.72 %
Strength increase	-	149.4kN	268.9kN
		71.0%	127.8%
Initial stiffness	35.6 kN/mm	68.0 kN/mm	76.2 kN/mm
Stiffness after 5cycles	11.2 kN/mm	22.2 kN/mm	26.5 kN/mm

3.2.5 Nominal shear strength expectataion

FIB Bulletin 24 and Eurocode 8 suggested that the nominal shear strength for concrete jacketed RC column can be evaluated assuming the composite section as unified. Strength expressions are not suggested specifically. The nomional shear strength of UHPC jacketed column can be estimated with similar approach. Assuming unified section between RC and UHPC jacket, the shear strength is the summation of all the contributions. There are three factors for the shear strength contribution: RC core, jacket matrix, steel fibers. In the case of additional stirrups inserted, their contributions should also be summed up. Therefore, the nominal shear strength, V_d can be calculated by

$$V_d = V_{core} + V_{jm} + V_{jf} + V_{js} \tag{8}$$

where, V_{core}, V_{jm}, V_{jf}, V_{js} are RC core, matrix, fiber and stirrup contributions, respectively. V_{core} and V_{jsd} can be calculated by ACI code provision. UHPC maxtix and fiber contributions can be calculated by adjusting expressions in K-UHPC design guideline. It suggests that $V_{jm} = 0.18\sqrt{f_{cd}}\,b_j d_j$ and $V_{jf} = (f_{sd}/\tan\beta_u)b_j z$, where f_{cd} is design compressive strength of UHPC, f_{sd} is design average tensile strength in the direction perpendicular to diagonal tension crack of UHPC, b_j is width of jacket, d_j is effective depth, β_u is angle occurring between axial direction and diagonal tension crack plane and is limited to $30°$, z is distance from the position of the resultant of the compressive stresses to the centroid of tensile steel (mm), generally $d/1.15$. Herein, strength reduction factors were not considered.

By the process explained above, nominal shear strength of test specimens can be calculated. In Fig. 3-16 to Fig. 3-18, the dotted lines represent the theoretical nominal shear strength. The calculated nominal strengths, V_d were found to be a little bit higher than maximum experimental results. However, the differences are small and considering the strength reduction factor, they are within allowable levels.

Detail calculation results are summarized in Table 3-7 including all contributions with experimental results. The ratio of V_d to V_{exp} were found to be around 1.1, which means 10% errors. Thus, it coud be considered that the shaer strength expression of equation (8) shows quite good expectations. However, as the number of specimens that could be compared is restricted to only two, the validity of equation (8) as a shear strength expression needs additional verifications.

Table 3-7 Nominal shear strength of UHPC jacketed column

	V_{core}	V_{jm}	V_{jf}	V_d	V_{exp}	V_d/V_{exp}
R-0	212	-	-	212.0	210.4	1.01
R-30	212	36.3	142.2	390.5	359.8	1.08
R-50	212	64.8	254.0	530.8	478.9	1.11

(Unit : kN)

3.2.6 Collapse mechanism

There are two types of diagonal cracks in RC structural members. One is shear compression crack and the other is diagonal tension crack. Considering that the diagonal cracks in rotrofitted specimen (R-30, R-50) start around the center of the column, not the point of load, and the shape of the cracks was far from compressive rupture, this crack is identified as a diagonal tension crack.

If assuming UHPC as homogeneous material, the diagonal tension crack would occur when the principal tensile stress in UHPC jacket reaches over the tensile cracking strength of UHPC. Therefore, it is necessary to find out principal stress distribution in the jacket in order to analyze the failure modes of test results.

3.2.7 Strain of transverse re-bars

Fig. 3-23 (a), (b) and (c) show strains of stirrup bars that are located fourth from the bottom stub for R-0, R-30 and R-50, respectively. In R-0 specimen, the strain hase kept in linear elastic state and suddenly went up at last cycle. This indicates that the column failed in very brittle manner. For R-30 and R-50 specimens, they showed similar behaviors. Before diagonal crack occurred, the strains have kept in linear elastic state, which means that there were not notable cracks in core concrete and diagonal crack has just occurred in UHPC jacket. Even after diagonal cracks occurred in jacket, the graphs show continuous linear state. However, after a few cycles, the strains rose up abruptly. It seems that as the diagonal cracks expanded the confinement effect from the jacket lost and sudden cracks must have occurred in core column.
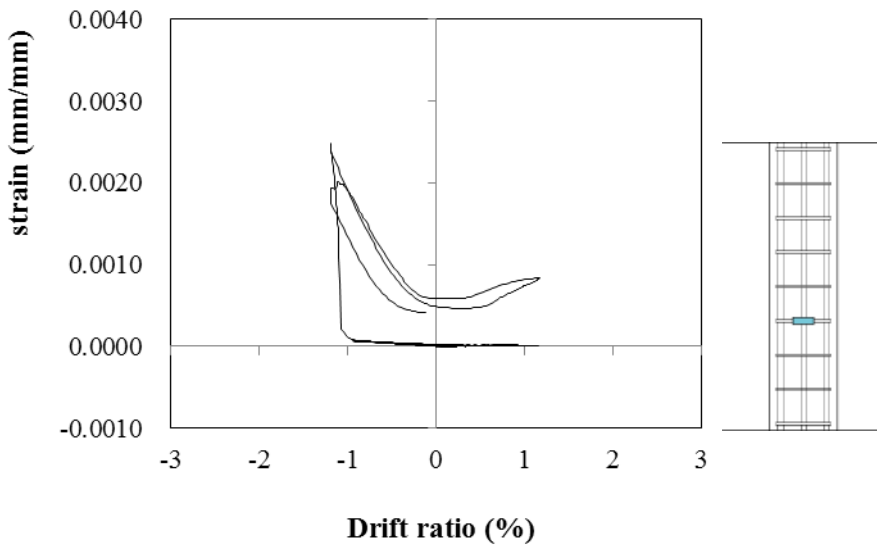
(a) R-0

Fig. 3-23 Strain of tie bars in core column
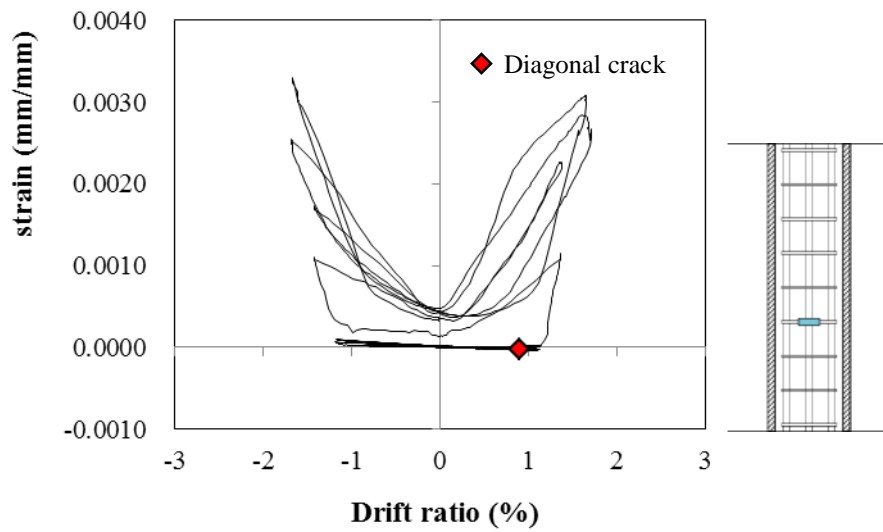
(b) R-30

(c) R-50

Fig. 3-23 Strain of tie bars in core column

3.2.8 RC column retrofitted by 50mm jacket and stirrups (R-50S)

The load-displacement curves and the cracks of R-50S reinforced with shear reinforcement (D10 @ 150) in addition to UHPC of 50mm are shown in Fig. 3-25. At 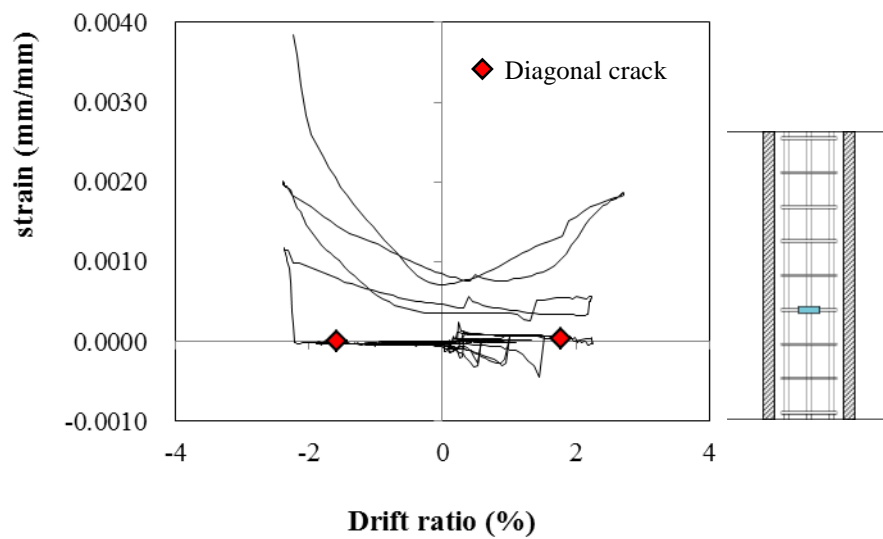a glance, it shows a clear difference from previous specimens. While R3 and R5 specimens failed by massive diagonal crack, in R5S specimen, although the diagonal crack occurred, it did not grow up to massive scale. The shear cracks generated at the early stage seems to be sustained by shear reinforcement so that cracks could not extend. As the jacket kept surrounding the core column and making it as a unified section, columns could be prohibited from shear failure and very ductile behavior was observed.

However, as resultant strength and stiffness of the column was much stronger than that of the base stub, and the cracks occured in the base continued to spread and open. The increase of lateral displacement gave rise to the shear deformation and bending deformation of the column. However, the flexural deformation itself concentrates on the joint and the column acted like rigid body while pushing the base. As a result, the cracks of the base absorbed a considerable amount of deformation energy and the column itself only repeated rigid body motion. The experiment was terminated after the deformation to 10% drift ratio.

The maximum lateral load was 480kN, which is slightly larger than that of R5 specimen. This satisfied the fact that both columns reached yield points and the flexural moments of both columns were same.
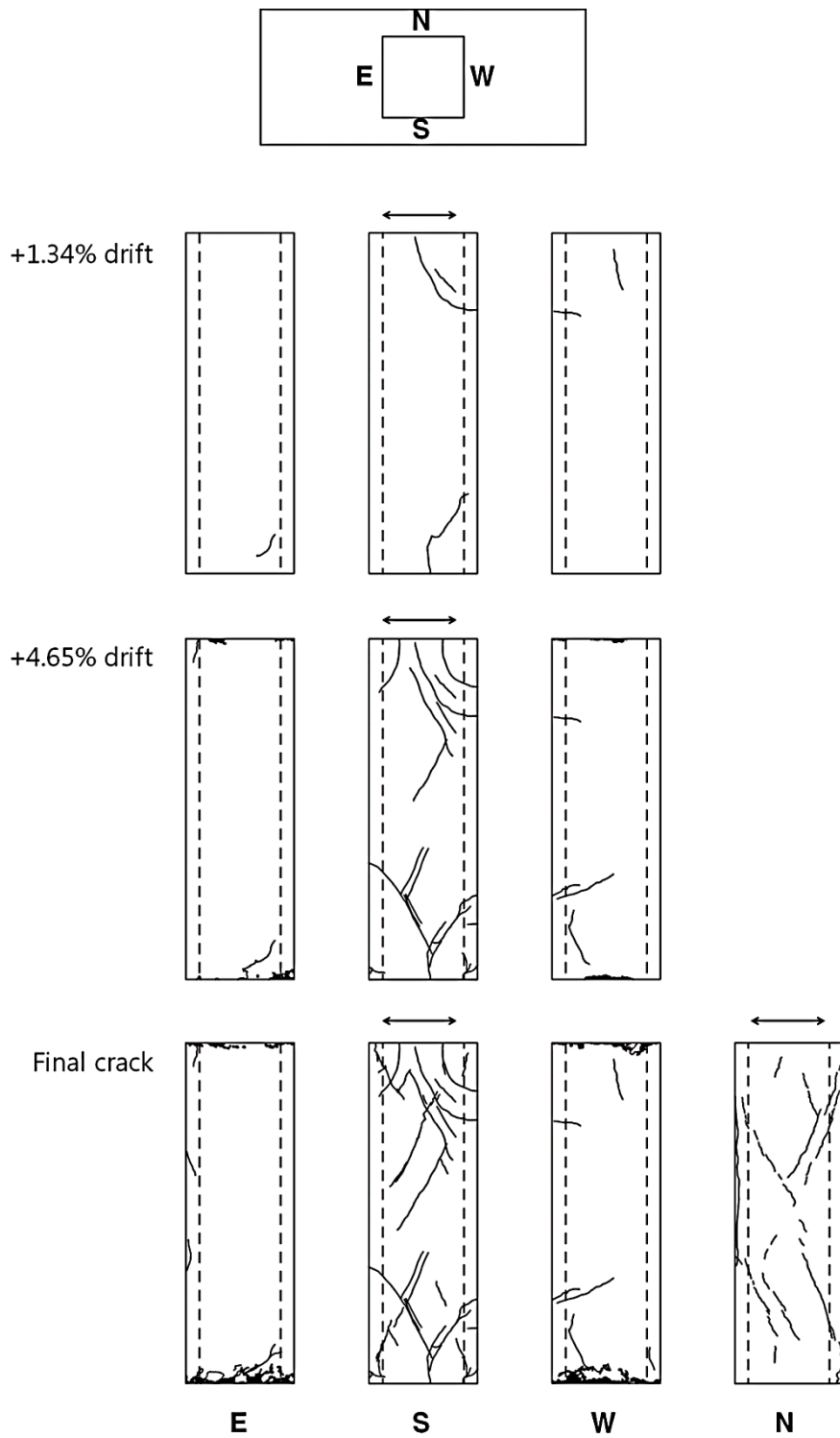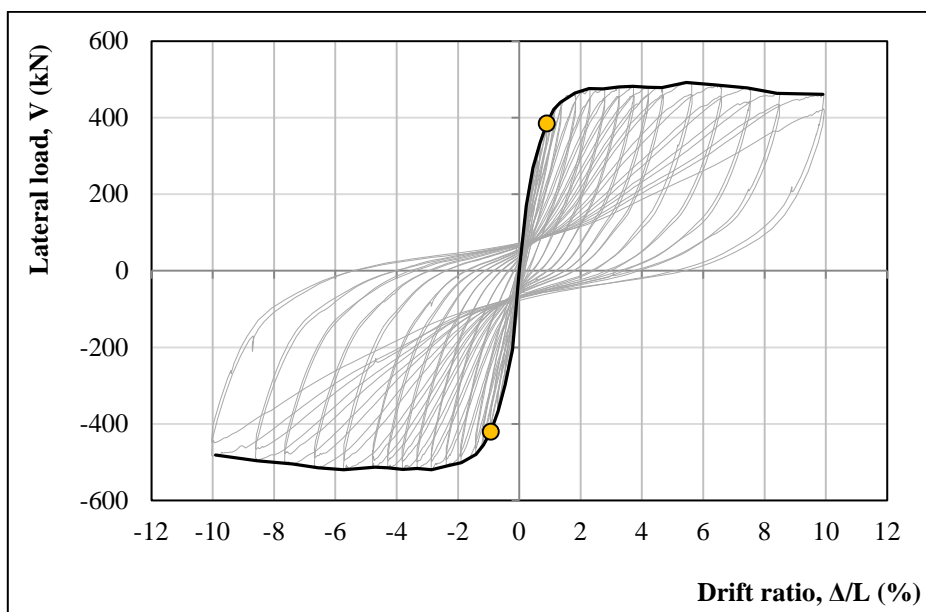
Fig. 3-24 Crack pattern (R-50S)

Fig. 3-25 Load-displacement curve (R-50)

Fig. 3-26 Base crack after experiment

Fig. 3-27 Rocking state of R-50S

It was confirmed that the column height increased from 1260mm to 1270mm by 10mm after the experiment. In the case of the general column lateral force test, the displacement after the flexural yielding should increase, and the tensile fracture of the reinforcing bar due to the compression of the concrete at the compression zone or the tensile failure at the tension zone should occur. However, the compressive strength of the UHPC is only marginal, It was judged that the maximum strain was not reached even at 10% drift due to occurrence of many slip in the repeated force.

Fig. 3-28 shows the strain of tie bars inserted in UHPC jacket. The graphs show obvious tendency that the strain was increasing linearly with drift ratio after a certain point. At 10% drift ratio, the maximum strain of RS-5 bar came out to be about 0.002mm/mm, which is a little bit lower than yield strain of reinforcement. This means that if the test had kept proceeding, the RS-5 tie bar would have yielded within a few cycles. While the strain graph of RS-5 which is located at around mid-height shows very symmetric shape, the strain of RS-1 that is put in near the stub shows unsymmetric tendency.
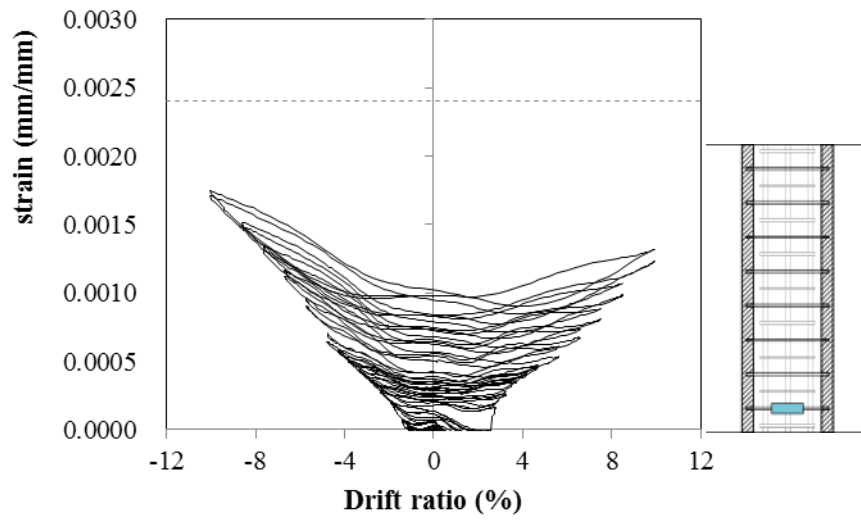
(a) JS-1
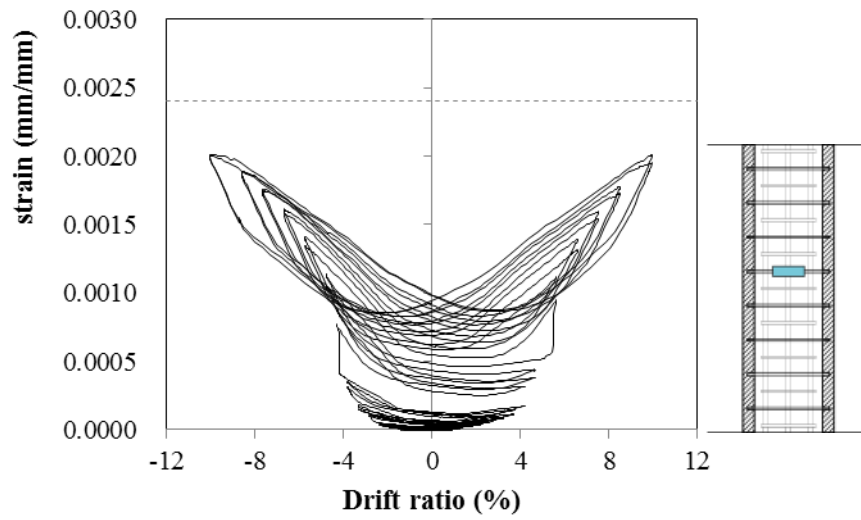
(b) JS-5

Fig. 3-28 Strain of tie bars in UHPC jacket

Fig. 3-29 shows the value of strain gages of tie bars along the height at the maximum drift ratio from 0.5% to 9.0% corresponding to each cycle. There are some points that can be inferred from these graphes.

First, it was found that the initial strains of JS-1 and JS-8, which are located near the end stubs, had negative values. This means that the tie bars around the column ends got negative strain at early stage. Normally, when the RC flexural members get lateral load, their stirrup ties get tensile stress and thus, should get positive strains. This is the effect of compressive strut that might have been formed around end stubs and this arch action governs the initial behavior over the beam action.

Second, there are obvious tendency that as drift ratio increases, strains of JS-1, JS-8 increase much faster than JS-4 and JS-5, which are located at inner part. And when drift ratio got very high, strains of inner tie bars became larger than boundary stirrups. This indicates that when lateral load is applied to this column, shear deformations are first concentratated near the end stubs and then gradually expand to inner parts as the drift ratio get futher higher. It is required to design shear stirrups of UHPC jacket depending on design seismic load. If the column is expected to get mid-range seismic deformation, strengthening end parts are more important. And if the column is expected to get severe seismic deformation, strengthening mid-parts would be more important.
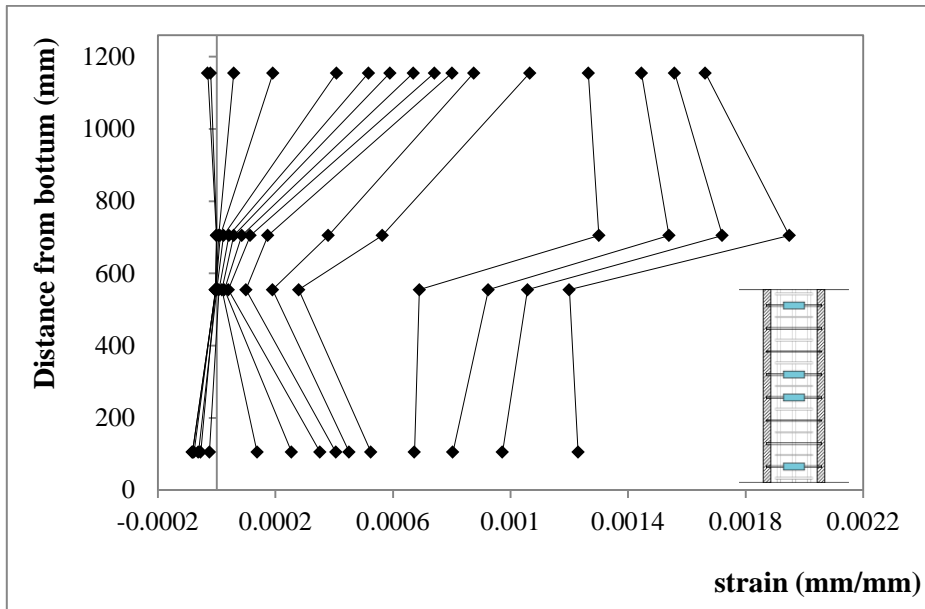
(a) positive direction (drift ratio : 0.5%~9.0%)
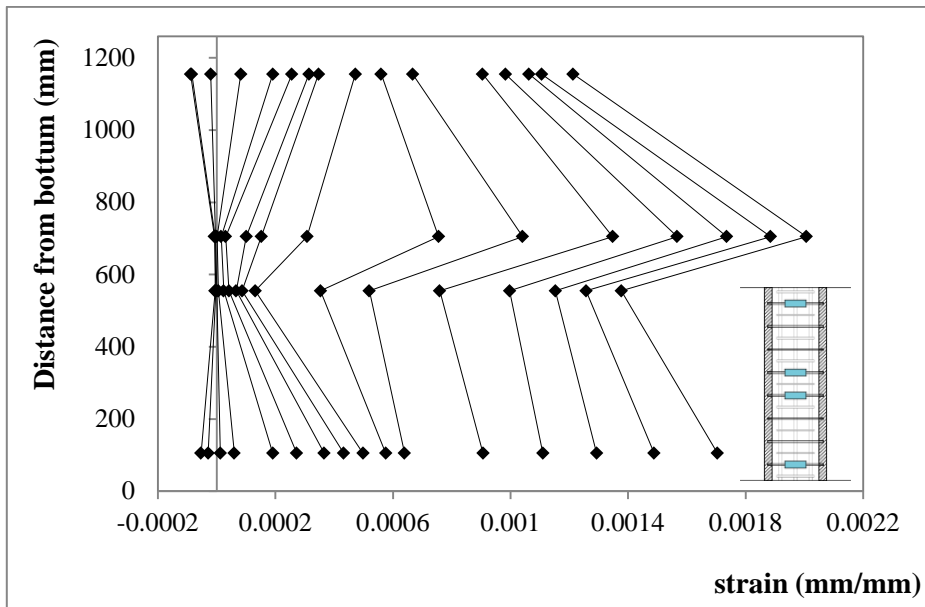
(b) negative direction (drift ratio : 0.5%~9.0%)

Fig. 3-29 Strain of tie bars along the height

Chapter 4. Theoretical Analysis

4.1 Introduction

4.1.1 General procedure

General analysis procedure is based on failure mode analysis just as the procedure to estimate design strength of RC column in. In chapter 3.1.3, failure curves for flexural compressive failure of which failure criteria is $\varepsilon_c = 0.003$ and shear failure based on code provision were plotted in the interaction diagram regarding to axial load, P and lateral load, V. Then, the lower curve depending on axial force will govern the failure mode.

The same approach was applied for the retrofitted composite column section to estimate a failure mode and corresponding maximum lateral load resistance capacity. The possible failure modes were defined based on experimental crack patterns. Next, for each failure mode, corresponding faillure curves were plotted in P-V interaction diagram. Finally, lower bound curve of all failure curves will decide theoretical failure modes and corresponding maximum load, which means load resistance capacity.

Due to the characteristic of this composite section, it was found that the interface shear strength has a very important role to determine the mechanical behavior of the retrofitted column. So, although experimental variables does not include interface shear capacity, in theoretical analysis, interface shear strength was treated as important factors in some intepretations.

4.1.2 Analysis method

Instead of using a special computer analysis program, the analysis used a simple strain compatibility solution to calculate the stress distribution of the column. The axial force and moment applied to column section at a certain height can be calculated, and based on these axial force and moment, corresponding strain distribution can be calculated by strain compatibility method. Then, normal and shear stress distribution can be calculated from the strain distributions. Finally, failure curve can be drawn by connecting the points in which the stresses reach failure criteria of each failure mode.

4.1.3 Basic assumptions

The assumptions used for the analysis are as follows.

1) The strain distribution at each column section is linear.

2) Tensile forces are only transferred by reinforcement of core column.

These assumptions are required because there is no physical connection beteen the UHPC jacket and concrete stub as illustrated in Fig. 4-1. Accordingly, UHPC doest not get direct tensile forces. Therefore, the vertical tensile stress of UHPC is assumed to be zero.

3) P-Δ effect was not considered

This study focuses only on the lateral load resistance capacity. Assuming lateral displacement is not large, P-Δ effect can be ignored.

4) Confinement effect of the jacket can be ignored.

Normally, jacketing method causes confinement effect to core column. However, in this case UHPC jacket contributes for strengthening the column mainly by supporting the external loads directly. Strengthening effect by confinement would be relatively very small compared to direct supports of the jacket. Moreover, confinement effect of the jacket in rectangular section is very difficult to estimate. Thus, most researches on confinement effect depend on experiments focusing on confinement effect, which is not the case. Therefore, Confinement effect was not considered in this study.
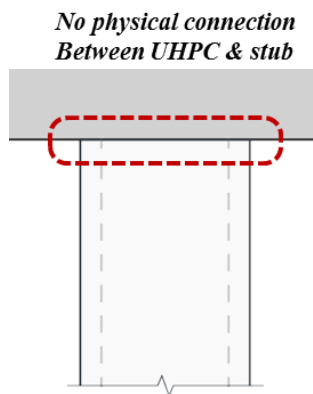

Fig. 4-1 Jacket connection to stub

4.2 Failure mode analysis

4.2.1 Failure mode classification
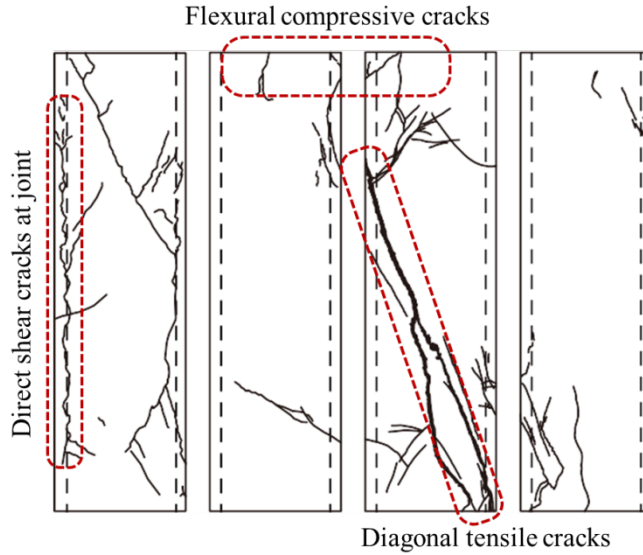
Fig. 4-2 Crack types of experiment result (R-30)

Three failure modes were considered in this study. Mode ① is a flexural compressive failure at column ends. This mode will happen when the strain of extreme compressive fiber(ε_{cm}) reaches UHPC's ultimate compressive strain(ε_{uu}).

Mode ② is a direct shear failure between web and flange of the jacket. As the composite section has higher stiffness outside and lower stiffness inside, the normal forces applied to outer jacket would be very large. It leads to high shear stress between the flange and web of the jacket and could give rise to this kind of failure mode when the direct shear stress(τ_{jt}) between web

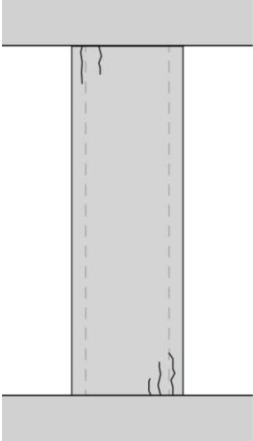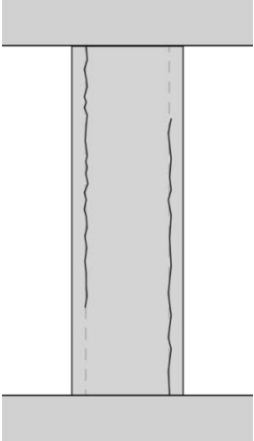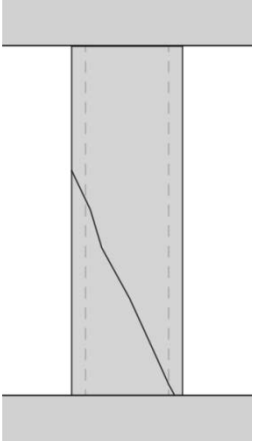and flange reaches over the shear strength($\tau_{u,allow}$) of UHPC.

Three failure modes were considered in this study. Mode ① is a flexural compressive failure at column ends. This mode will happen when the strain of extreme compressive fiber(ε_{cm}) reaches UHPC's ultimate compressive strain(ε_{uu}).

Mode ② is a direct shear failure between web and flange of the jacket. As the composite section has higher stiffness outside and lower stiffness inside, the normal forces applied to outer jacket would be very large. It leads to high shear stress between the flange and web of the jacket and could give rise to this kind of failure mode when the direct shear stress(τ_{jt}) between web and flange reaches over the shear strength($\tau_{u,allow}$) of UHPC.

Mode ③ is a diagonal tension failure in the web plane, which is the failure modes of the actual tests. This mode will happen when the principal tensile stress(σ_1) in the jacket reaches over the tensile strength($f_{u,t}$) of the UHPC. This mode is also influenced by the composition of the section, becuase the principal tensile stress is highly affected by the shear stress of the web.

There are other possible failure modes such as UHPC's tensile failure due to hoop stresses by confinement effect or shear failure of internal core. Further studies are required to deal with these failure modes.

Table 4-1 Failure mode classification

	Mode ①	Mode ②	Mode ③
Failure mode	Compressive failure of UHPC	Direct shear failure between web-flange	Diagonal tension failure in web plane
Crack patterns			
Failure criteria	$\varepsilon_{cm} = \varepsilon_{uu}$	$\tau_{jt} = \tau_{u,allow}$	$\sigma_1 = f_{u,t}$

4.2.2 Flecxural compressive failure at column ends

P-V interaction curve for mode 1 can be drawn by transforming P-M interaction diagram. P-M interation curve can be found out from strain compatibility solution. The process is almost same as with chapter 3.1.3. The difference is that first, the strain of the maximum compressive fiber is $\varepsilon_{uu} = 0.004$, instead of $\varepsilon_{cu} = 0.003$. Second, as the maximum strain of the

concrete is not always $\varepsilon_{cu} = 0.003$, the equivalent stress block method cannot be applied. Thus, the stress-strain curve of concrete was assumed as a double-linear curve described in Fig. 4-3. The maximum compressive strength and the initial stiffness were based on material experimental result.
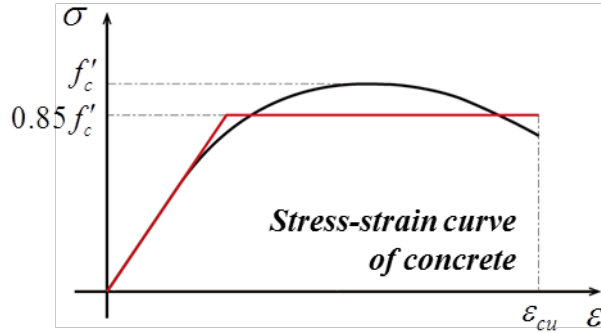
Fig. 4-3 Assumed stress-strain curve of concrete

The process is simply illustrated in Fig. 4-4. While varying the neutral axis c, the sectional force and moment can be plotted and the resultant P-M curve is shown in Fig. 4-5. If there is no P-Δ effect as assumed, the maximum moment in column should satisfy equation (9) for double curvature column. Thus, the lateral load, V has linear relation with moment, M. Therefore, P-V interaction diagram can be directly drawn from the P-M curve.

$$M = \frac{VL}{2} \tag{9}$$
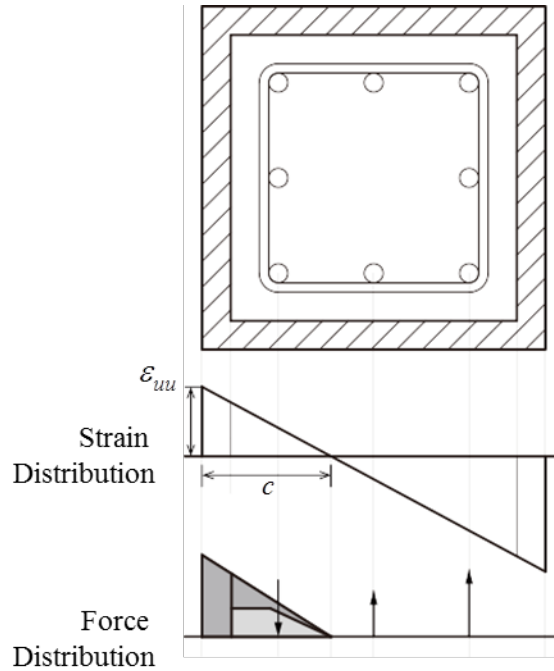
Fig. 4-4 Strain compatibility solution for composite section

Fig. 4-6 shows the failure curves of flexural failure mode for the jacketed columns including for the unjacketed section. The lateral load capacity increased about two times at zero axial load and the axial load capacities are calculated to increase about 2.5 to 4 times depending on the jacket thickness.
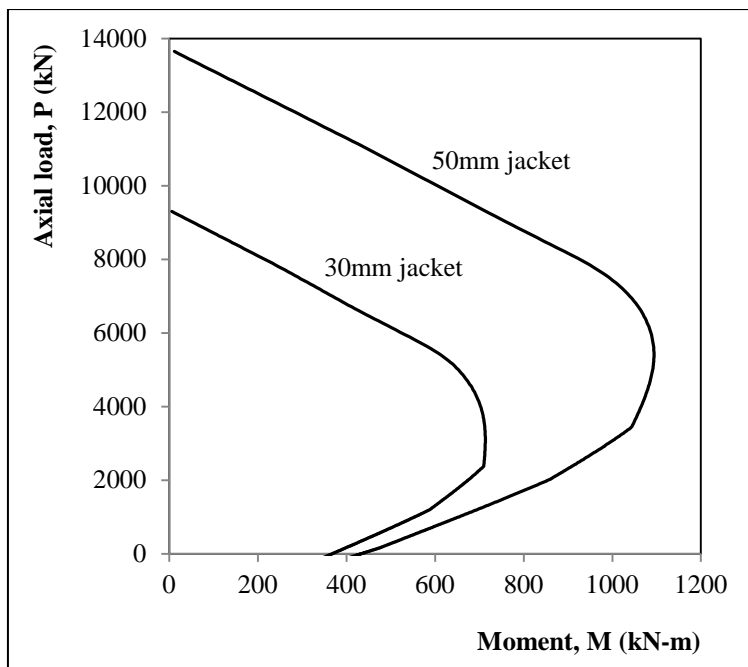
Fig. 4-5 P-M interaction diagram for jacketed section
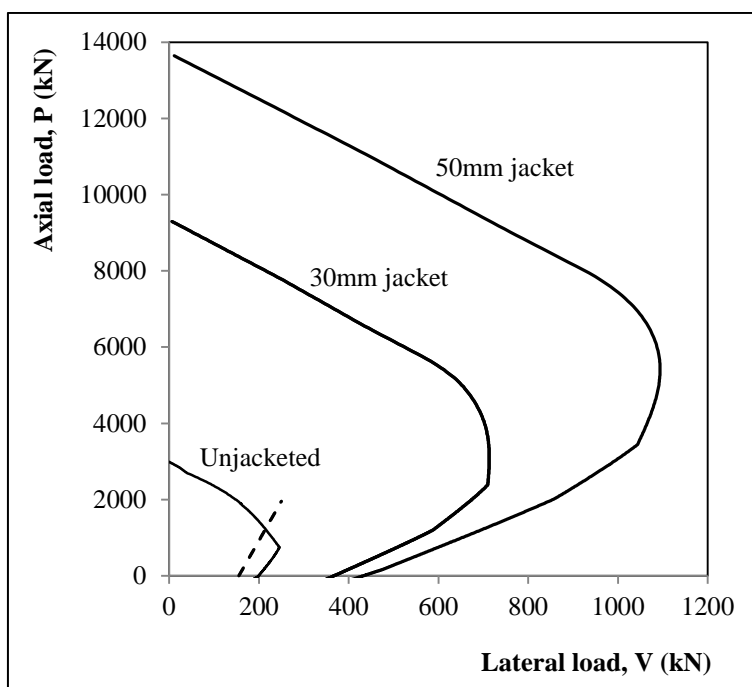
Fig. 4-6 P-V interaction diagram (failure mode 1)

4.2.3 Direct shear failure between web-flange of UHPC jacket
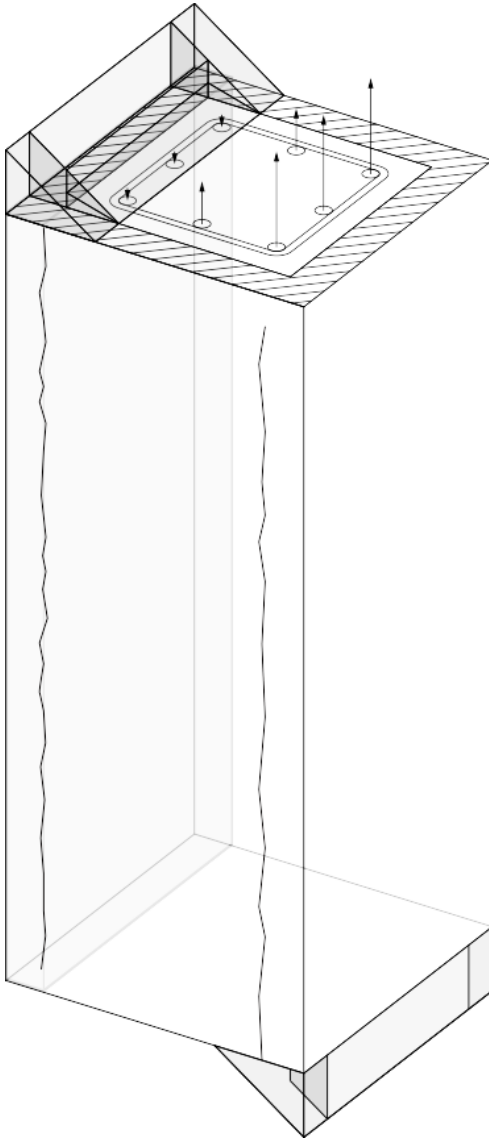
Fig. 4-7 crack patterns of mode 2 and normal stress distribution at end
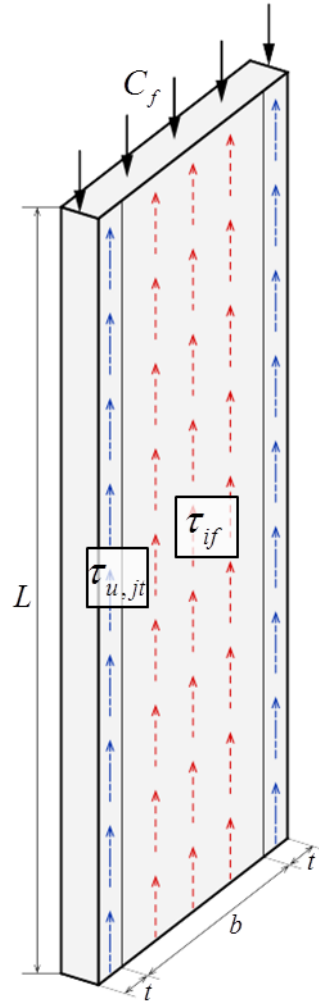
Fig. 4-8 vertical stress distribution in flange

Second failure mode is a direct shear failure between web and flange of UHPC jacket. Fig. 4-7 shows the crack patterns of this failure mode and normal stress distribution at column end when lateral load or moment appliy

to the column. This failure mode could occur when the direct shear stress in web-flange joint is higher than shear strength of UHPC.

Interface shear strength should be considered to analyze this failure mode. If interface shear strength is sufficiently large (case (a)), the shear flow caused by C_f could be directly transferred aligned with the direction of shear force (Fig. 4-9. (a)). In this case the shear stress among the interface could be regarded same (equation (27)). However, if interface shear strength is not sufficient (case (b)), the shear stress in flange should be transferred to web to fill the insufficient amount (Fig. 4-9. (b)). This additional shear stress will increase the shear stress in web and hasten this shear failure mode.
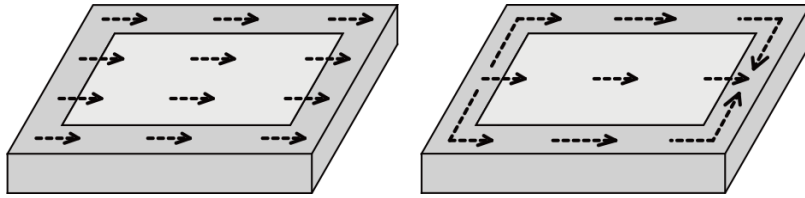
Fig. 4-9 shear flow in column section:

a) if $\tau_{if,allow}$ is large enough, b) if $\tau_{if,allow}$ is not sufficient

The shear stress at joint can be calculated from the vertical force equilibrium in Fig. 4-8.

In the case of $\tau_{if,allow} \geq \dfrac{C_f}{(b+2t)L}$

$$\tau = \tau_{if} = \tau_{u,jt} \qquad\qquad\qquad \textbf{(10)}$$

$$C_f = \tau(b + 2t)L \qquad \qquad \textbf{(11)}$$

$$\tau_{u,jt} = \tau = \frac{C_f}{(b+2t)L} \qquad \qquad \textbf{(12)}$$

In the case of $\tau_{if,allow} < \dfrac{C_f}{(b+2t)L}$

$$\tau_{if} = \tau_{if,allow} \qquad \qquad \textbf{(13)}$$

$$C_f = \left(\tau_{if,allow}(b) + \tau_{jt}(2t)\right) \cdot L \qquad \qquad \textbf{(14)}$$

$$\tau_{u,jt} = \frac{C_f/L - \tau_{if,allow}b}{2t} \qquad \qquad \textbf{(15)}$$

where,

$\tau_{if,allow}$ = allowable interface shear stress (MPa)

τ_{if} = interface shear stress (MPa)

$\tau_{u,jt}$ = direct shear stress at the joint (MPa)

C_f = Normal force applied to jacket flange (kN)

The failure critera would be $\tau_{u,jt} = \tau_{u,allow}$, where,

$\tau_{u,allow}$ = allowable shear stress of UHPC (MPa)

For the analysis above, the interface shear strength, $\tau_{if,allow}$ and direct shear

strength of UHPC, $\tau_{u,allow}$ are required to be estimated. As explained in chapter 2.3, the interface shear strength has three contributions: cohesion, friction, clamping. In the experiment, the clamping bars were not used, so the clamping factor does not have to be considered. Also, there is no force normal to interface. Thus, the friction factor doesn't need to be considered as well. Therefore, only cohesion factor needs to be considered.

The cohesion factor consists of cohesion coefficient and design value of concrete tensile strength. The value of cohesion coefficient, c for sandblasted surface could be estimated from (Santos et el, 2014).

From Fig. 4-10, cohesion coefficient is 0.93 and,

$$\tau_{if,allow} = c \cdot f_{ctd} = 2.23\text{MPa} \qquad \textbf{(16)}$$

As the values used for equation (16) have relatively large deviations, the interface shear strength was assumed conservatively as $\tau_{if,allow} = 2\text{MPa}$
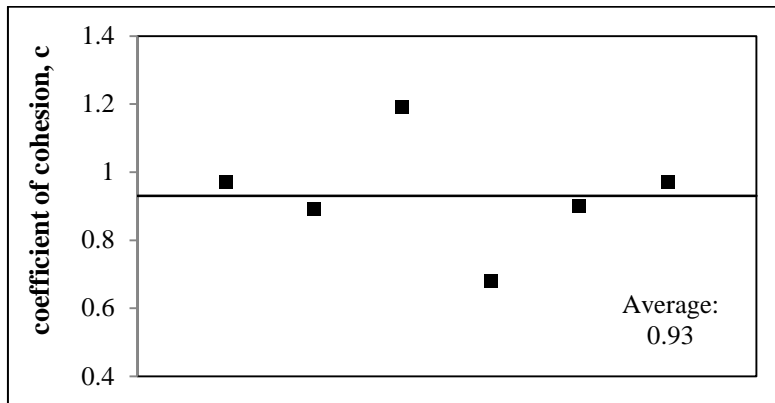

Fig. 4-10 Cohesion coefficient for sandblasted surface (Santos et el, 2014)

The direct shear friction strength of UHPC is explained in chapter 2.4. For the same reason with interface shear strength, the clamping factor and friction factor by normal stress need not be considered. The cohesion factor and friction by steel fiber contribution should be considered.

$$\tau_{u,allow} = \tau_c + \mu \, f_{u,ctd} \big/ K = 9.2 \text{MPa} \qquad \textbf{(17)}$$

For conservative analysis, assume

$$\tau_{u,allow} = 9 \text{MPa} \qquad \textbf{(18)}$$

Using the algorithm ofFig. 4-13, it is possible to get failure curve of mode 2. The resultant P-V interaction diagram for R-30 and R-50 sections are plotted in Fig. 4-11 and Fig. 4-12. For the interface shear strength of assumed 2MPa, it is shown that the failure curve for mode 2 in R-30 is almost same with mode 1 curve. In the case of R-50 section, failure curve for mode 2 is much lower than mode 1, which means that the column is apt to fail in mode 2 rather than mode 1.
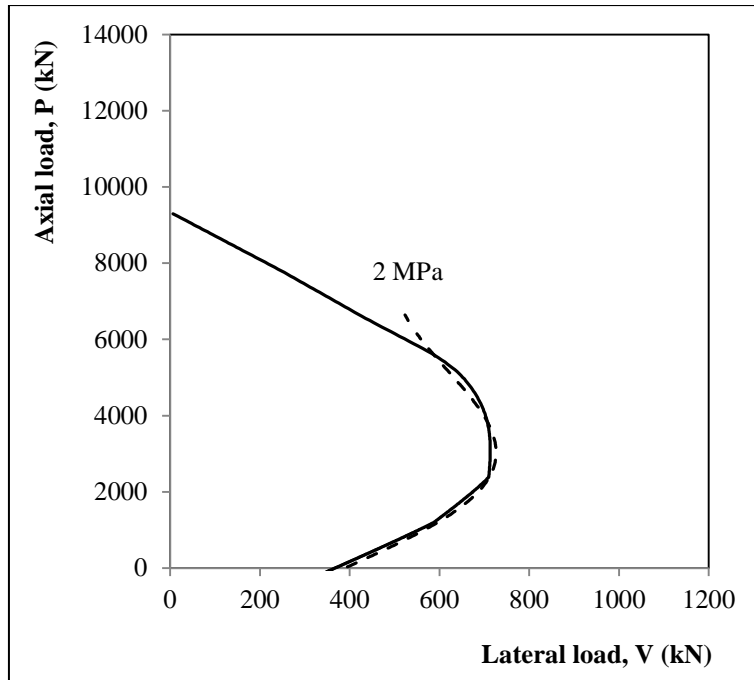
Fig. 4-11 P-V interaction diagram (30mm, mode 2)
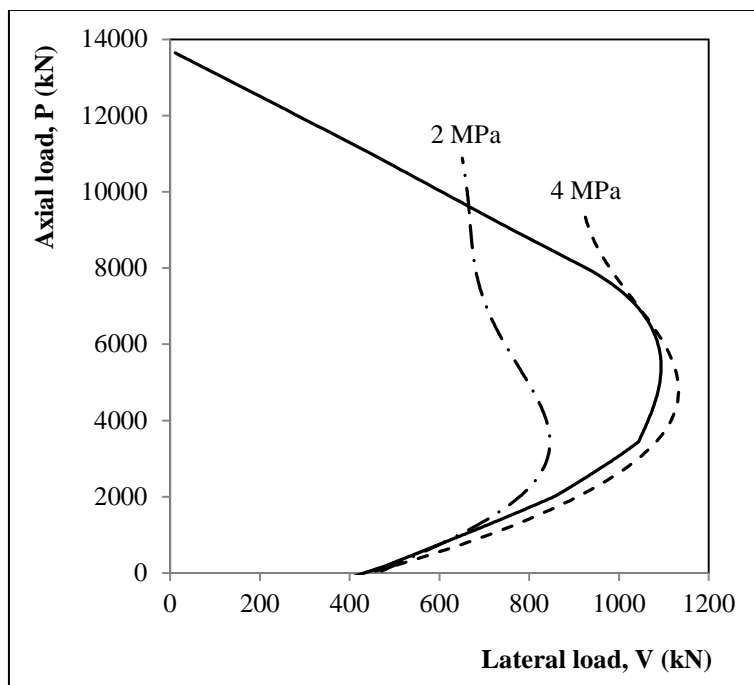
Fig. 4-12 P-V interaction diagram (50mm, mode 2)
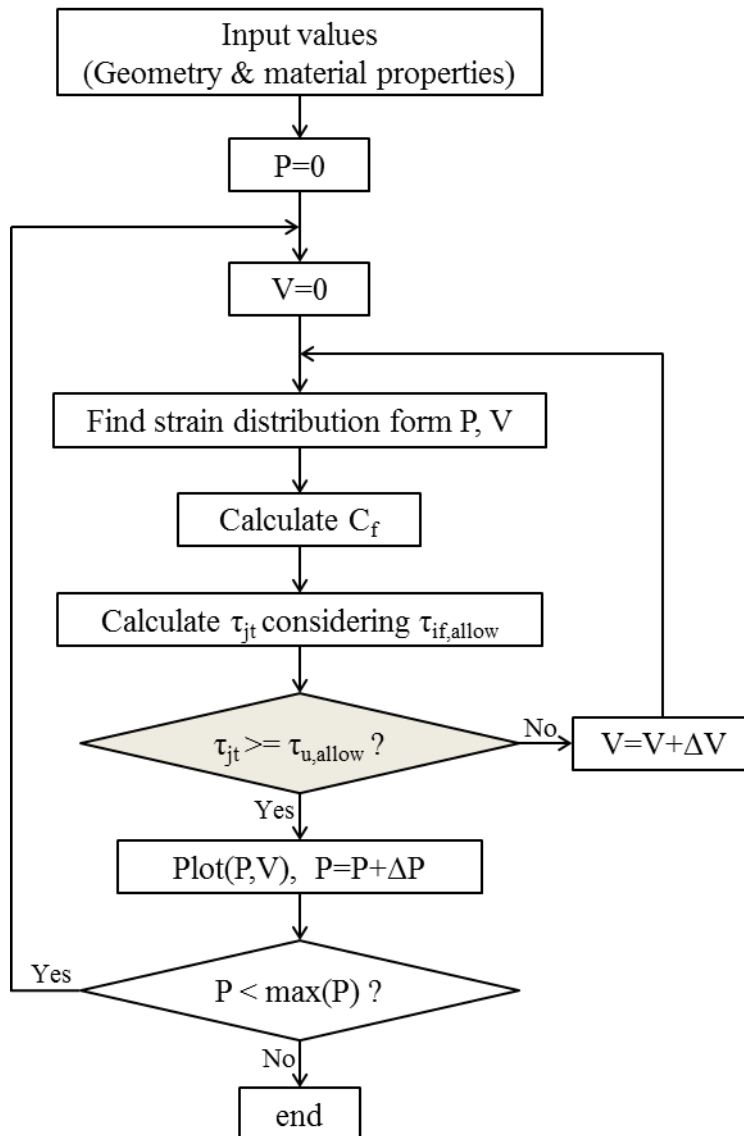
Fig. 4-13 Analysis method for failure mode 2

4.2.4 Diagonal tension failure in UHPC web

The third failure mode is a diagonal tension failure, which was the experimental result. Fig. 4-14 shows the crack patterns of this failure mode. This failure mode could occur when the maximum principal tensile stress in UHPC web is higher than tensile strength of UHPC, which may not be high enough.
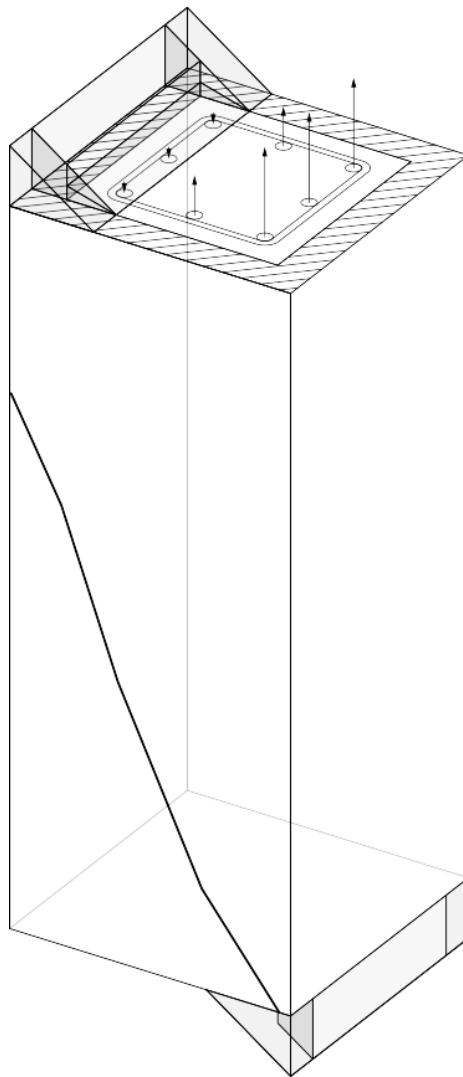
Fig. 4-14 Crack patterns of mode 3

It is necessary to analyze principal stresses among the UHPC web to find out the maximum value. For that purpose, the normal and shear stress at any location in the UHPC web should be estimated. As shown in Fig. 4-15, the axial force and moment at loacation z, can be found from the axial force and moment diagram, respectively. Then, it is possible to get strain distribution at height z, which is assumed to be linear. This strain distribution at z can be defined with two funtions, $\varepsilon_m(z)$ and $c(z)$ where $\varepsilon_m(z)$ is maximum compressive strain at extreme compressive fiber and $c(z)$ is the length between extreme compressive fiber and neutral axis. These are functions of z.

As the strain distribution at height z, defined by $\varepsilon_m(z)$ and $c(z)$, is given, the normal stress can be easily found out by multiflying elastic modulus of UHPC to strain distributions. As assumed in 4.1.3, the tensile stress is not considered. Thus, the negative value in the vertical stress should be just zero.

Fig. 4-15 Strain distribution at height z

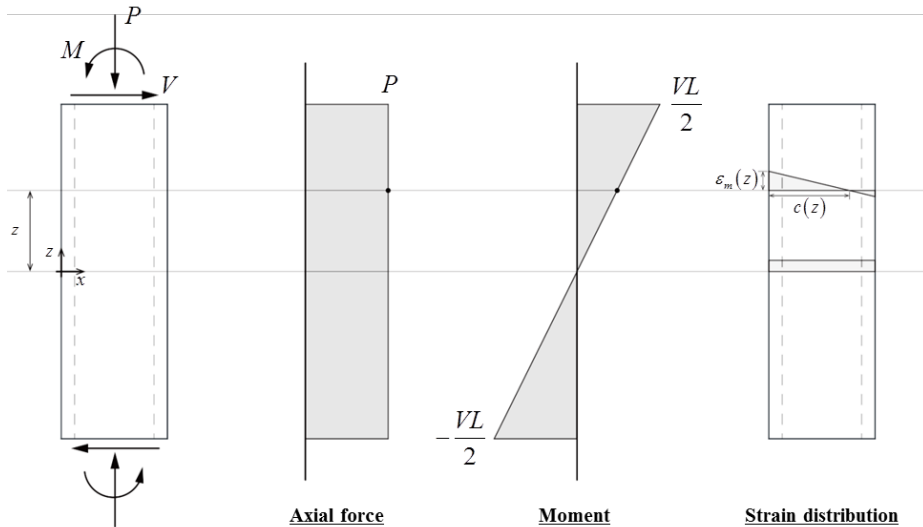The next step is to estimate the shear stress distribution. It can be estimated from the normal stress distributions applied to UHPC. The shear stress was divided to stress by normal force applied to web, C_w and shear stress by normal force applied to C_f.

Fig. 4-16 shows the normal stress distribution at (A) highlighting the web portions. The location (A) indicates where all the section get normal compressive strain. The shear stress by normal force should start with zero at left side and end with zero at right side. For simplicity, the shear stress distribution was assumed symmetric and accordingly, the net normal stress distribution was also assumed to be symmetric. Then, from the vertical force equilibrium in the free body diagram of Fig. 4-16, equation (19) and (20) can be built.

$$
\begin{aligned}
\tau_{jw}(z,x) \cdot t \cdot dz &= \left[\int_0^x \left(\sigma_m (z+dz) - \sigma_m (z) \right) dx \right] \cdot t \\
&= \left[\sigma_m (z+dz) - \sigma_m (z) \right] \left[\int_0^x \left(1 - \frac{2x}{(h+2t)} \right) dx \right] \cdot t \qquad \textbf{(19)} \\
&= \left[\sigma_m (z+dz) - \sigma_m (z) \right] x \left(1 - \frac{x}{(h+2t)} \right) \cdot t
\end{aligned}
$$

$$
\begin{aligned}
\tau_{jw}(z,x) &= \left[\frac{\sigma_m (z+dz) - \sigma_m (z)}{dz} \right] x \left(1 - \frac{x}{(h+2t)} \right) \\
&= \frac{d\sigma_m}{dz} x \left(1 - \frac{x}{(h+2t)} \right) \qquad \textbf{(20)} \\
&= E_U \frac{d\varepsilon_m}{dz} x \left(1 - \frac{x}{(h+2t)} \right)
\end{aligned}
$$

where,

τ_{jw} = Shear stress by C_w (MPa)

σ_m = Normal stress at extreme compressive fiber (MPa)

Equation (20) shows that the shear stress by C_w could be determined by, a derivative of maximum strain by height, z with other material and geometry factors.
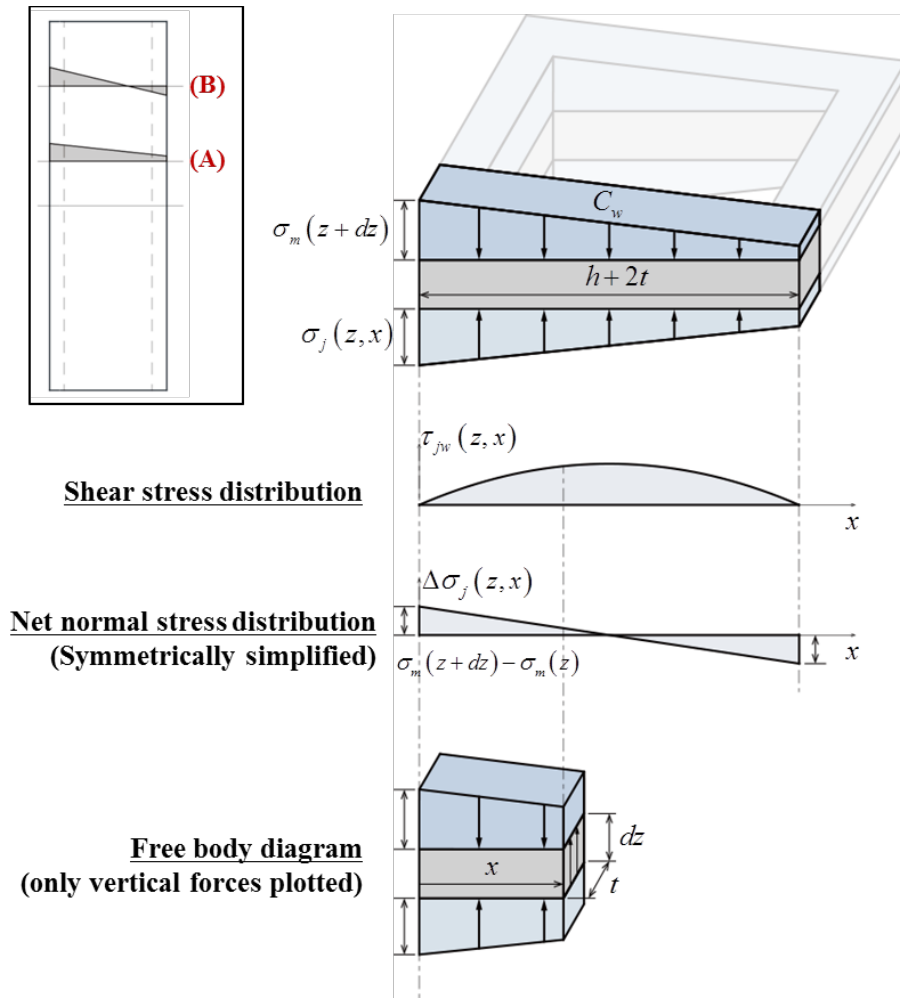
Fig. 4-16 Normal stress distribution by C_w in web at (A)

Fig. 4-16 shows the normal stress distribution at (B) which indicates the location where only part of the section gets normal compressive strain. The shear stress by normal force should start with zero at left side and end with zero at the point where normal stress becomes zero. Assuming shear stress distribution as symmetric, then, from the vertical force equilibrium in the free body diagram of Fig. 4-17, equation (21) and (22) can be built.

Fig. 4-17 Normal stress distribution by C_w in web at (B)

$$\tau_{jw}(z,x) \cdot t \cdot dz = \left[\int_0^x \left(\sigma_m(z+dz) - \sigma_m(z) \right) dx \right] \cdot t$$

$$= \left[\sigma_m(z+dz) - \sigma_m(z) \right] \left[\int_0^x \left(1 - \frac{2x}{c(z)} \right) dx \right] \cdot t \qquad \textbf{(21)}$$

$$= \left[\sigma_m(z+dz) - \sigma_m(z) \right] x \left(1 - \frac{x}{c(z)} \right) \cdot t$$
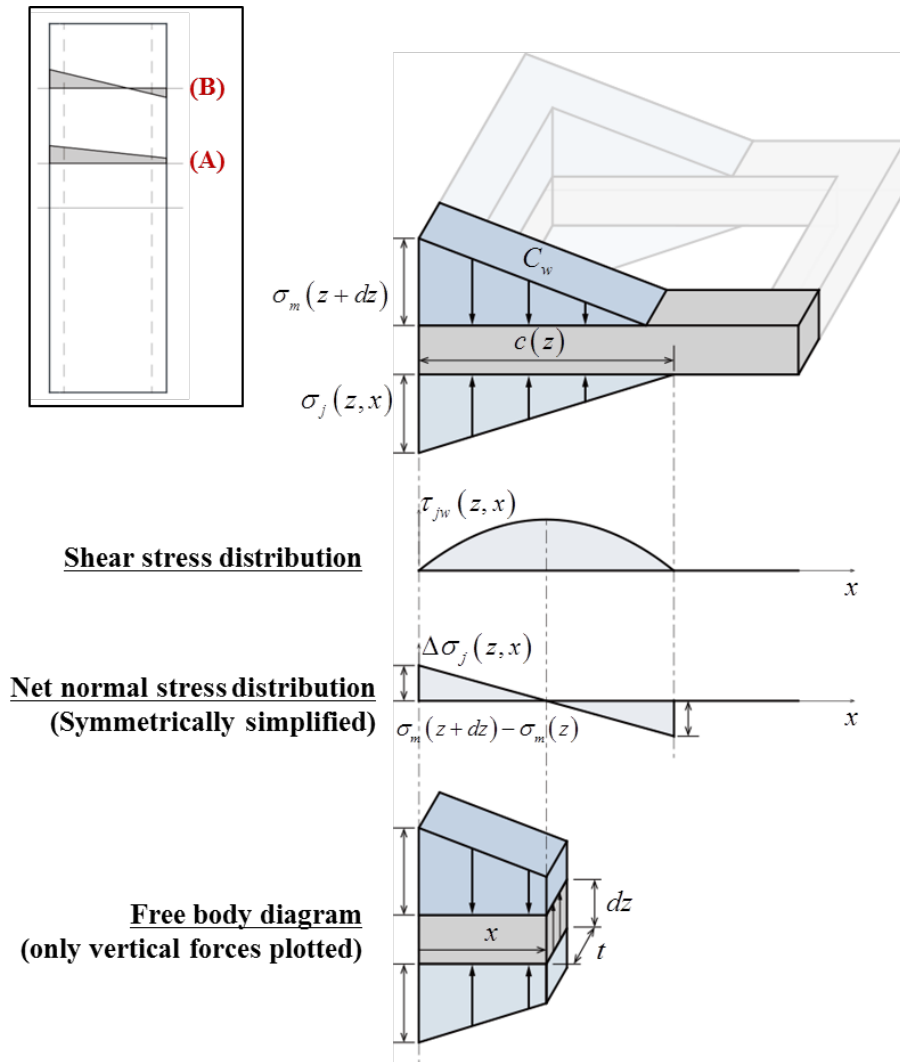
$$\tau_{jw}(z,x) = \left[\frac{\sigma_m(z+dz) - \sigma_m(z)}{dz} \right] x \left(1 - \frac{x}{c(z)} \right)$$

$$= \frac{d\sigma_m}{dz} x \left(1 - \frac{x}{c(z)} \right) \qquad \textbf{(22)}$$

$$= E_U \frac{d\varepsilon_m}{dz} x \left(1 - \frac{x}{c(z)} \right) \qquad \left(0 \le x \le c(z) \right)$$

The next step is to estimate shear stress in the web by normal force in flange, C_f. In the same as in 4.2.3, the interface shear strength need to be considered. As illustrated in Fig. 4-18, if interface shear strength is large enough (Fig. 4-18 (a)), there will be no shear flow toward the web. The shear stress by C_f at interface would be same as shear stress by C_w where $x = t$. Therefore,

If $\tau_{if,allow} \ge \tau_{jw}(z,t)$,

$$\tau_{if}(z) = \tau_{jw}(z,t) \qquad \textbf{(23)}$$

$$\tau_{jf}(z) = 0 \qquad \textbf{(24)}$$

However, if the interface shear strength is not sufficient, the shear flow toward the web would occur (Fig. 4-18 (b)).

If $\tau_{if,allow} < \tau_{jw}(z,t)$,

$$\tau_{if}(z) = \tau_{if,allow} \qquad (25)$$

$$\tau_{jf}(z) = \left(\tau_{jw}(z,t) - \tau_{if,allow}\right)\left(\frac{t}{b/2}\right) \quad (t \leq x \leq h+t) \quad (26)$$

where,

τ_{jf} = Shear stress in the web by C_f (MPa)

Equation (26) was built with a assumption that shear stress by Cf is uniform along the web.
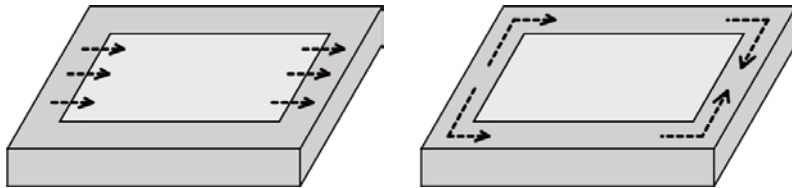
Fig. 4-18 shear flow of flange in column section:

a) if $\tau_{if,allow}$ is large enough, b) if $\tau_{if,allow}$ is not sufficient
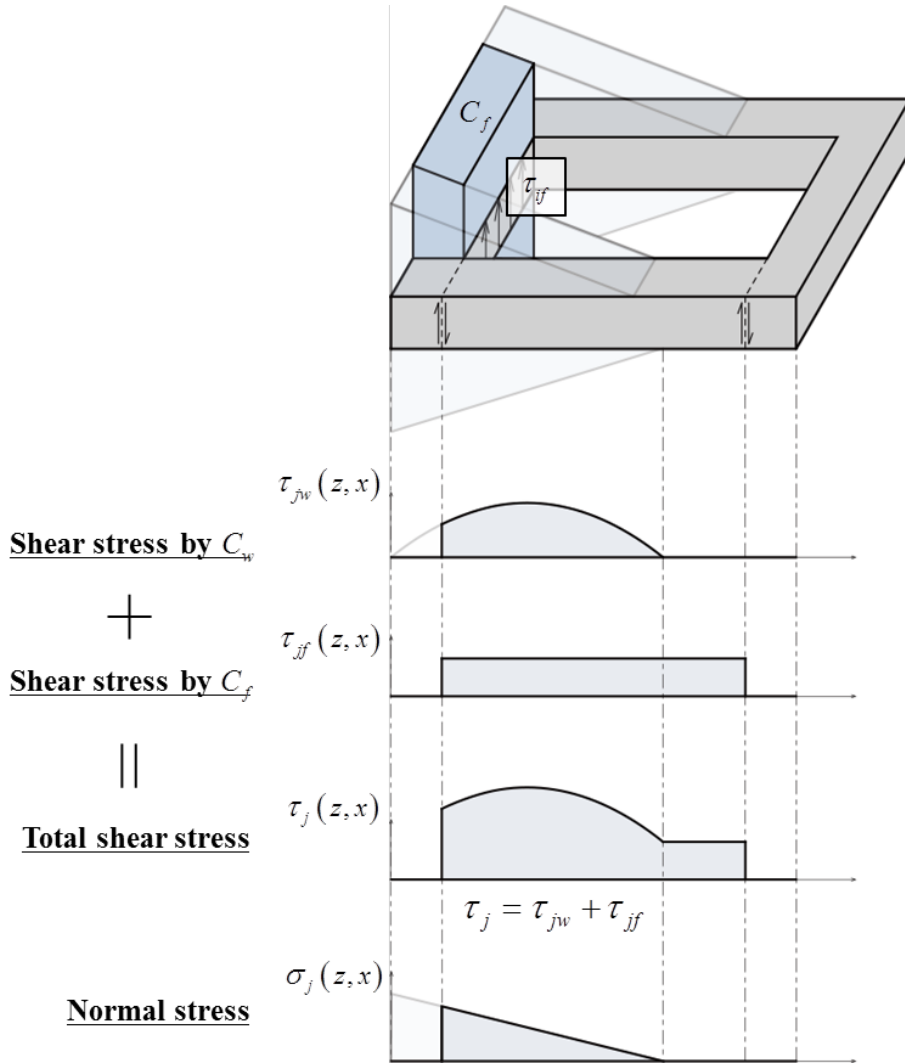
Fig. 4-19 Normal stress distribution by C_f in web

The total shear stress can be found by just adding τ_{jw} and τ_{jf}, as shown in Fig. 4-19. Then, as the shear stress and normal stress at any location in the web of jacket, the principal stress can be found out from the equation (27), which can be built from the Mohr's circle that is described in Fig. 4-20.
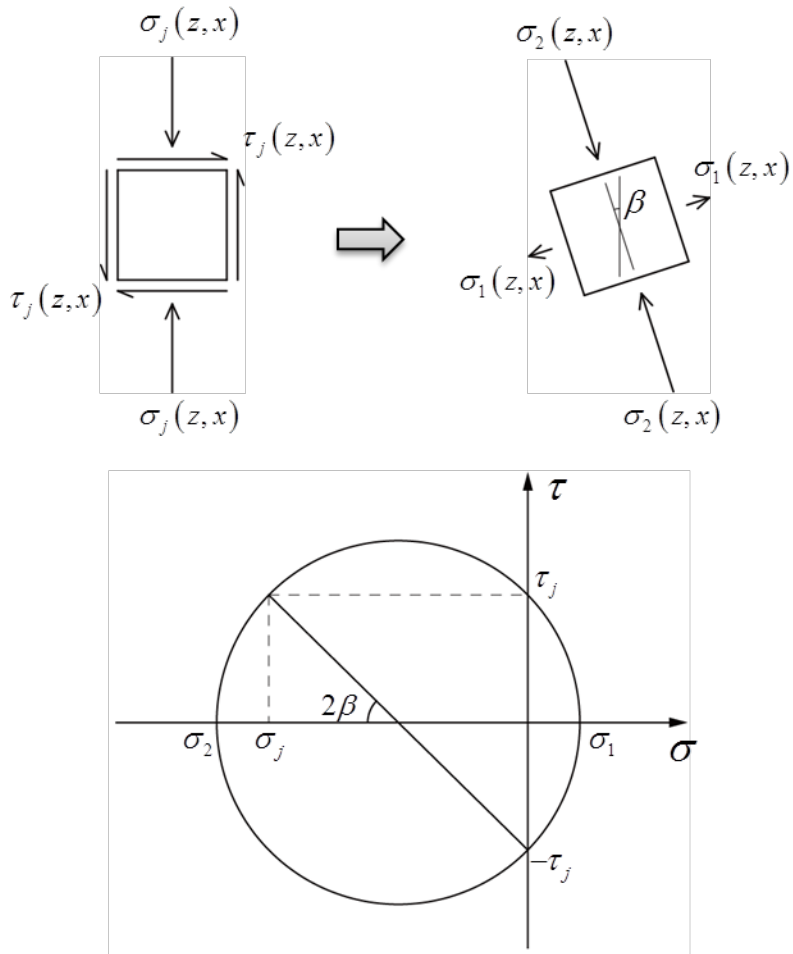
Fig. 4-20 Mohr's circle

$$\sigma_1 = \sqrt{\left(\frac{\sigma_j}{2}\right)^2 + \tau_j^{\,2}} - \left(\frac{\sigma_j}{2}\right) \tag{27}$$

$$\beta = \tan^{-1}\left(\frac{2\tau_j}{\sigma_j}\right) \tag{28}$$
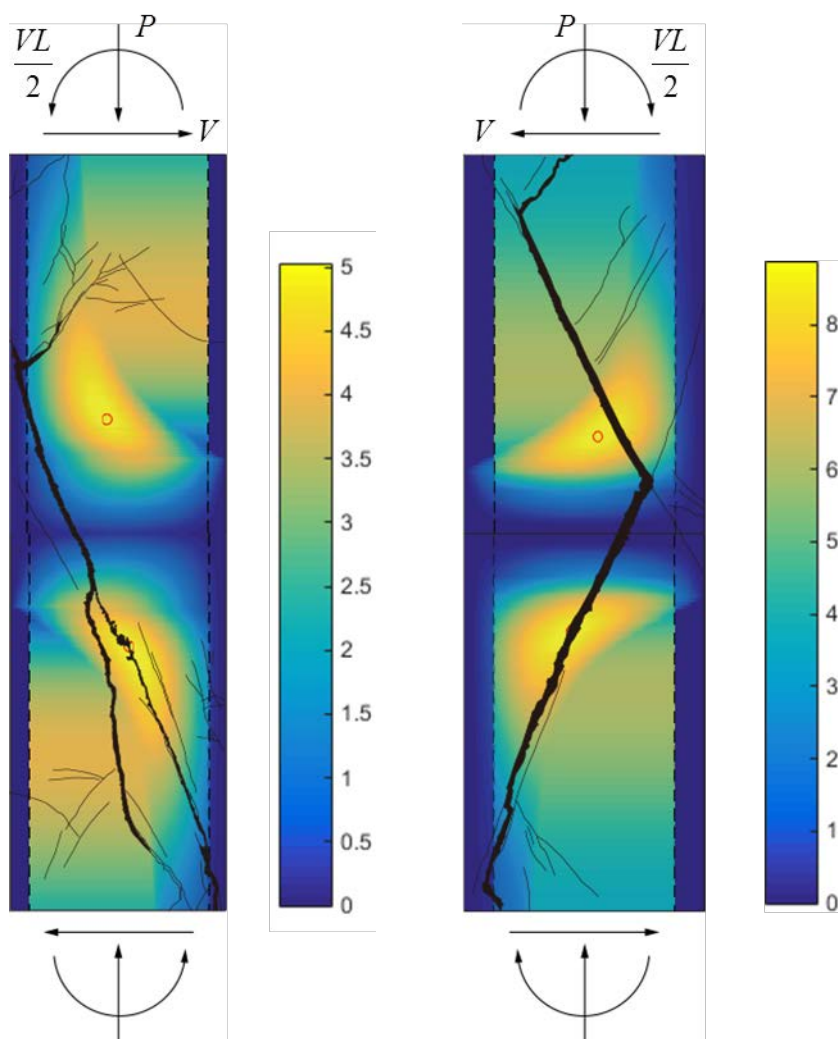
Fig. 4-21 Principal stress distribution at the cracking load
a) for R-30, b) for R-50

The principal tensile stress distributions of the experiment specimens (R-30, R-50) were estimated with this method at their cracking loads. The results are plotted in Fig. 4-21 with actual cracking patterns overlapped. The maximum principal tensile stresses appeared to occur at a little away from the middle of the column, while the principal stresses at centers were quite low.

This is because, a derivative of maximum strain by height, $d\varepsilon_m / dz$ which is the main factor of the shear stress (Equations (20), (22)), is lowest at the center.

The shapes and directions of the areas of high principal tensile stresses appeared to match with the actual crack patterns, which means that although there are many assumtions are used for this method, it can evaluate the principal tensile stress quite well in some degrees.

The maximum values of principal tensile stresses came out to be about 5.0MPa and 8.8MPa for R-30 and R-50, respectively. The cracks would occur when the area that has a principal tensile stress over the tensile strength of the UHPC become large to some extent. This extent is difficult to extimate. For simplicity and conservative analysis, just assume that the column could fail in diagonal crack when the maximum principal tensile stress at a point reaches the tensile strength of UHPC.

Applying above process, the P-V interaction diagram was plotted with an algorithm described in Fig. 4-22. The resultant diagrams are shown in Fig. 4-23 and Fig. 4-24. For comparision, the interface shear strengths for 5MPa 10MPa are plotted altogether as well as for 2MPa.

The result shows that the failure curve for mode 3 is much lower than mode 1 when axial load is not that much high. This means that this composite column is prone to fail in diagonal tension cracking failure rather then flexural compressive failure. When the interfacet shear is large enough (about 10MPa), then, the failure cure for mode 3 is almost get out of the failure curve of mode 1. Therefore, if it is necessary to secure high lateral load capacity in normal

axial load condition, while utilizing the high compressive strength of UHPC, the interface shear strength need to be designed high enough. This can be accomplished by adding some clamping bars at the interface as well as surface roughening treatment.
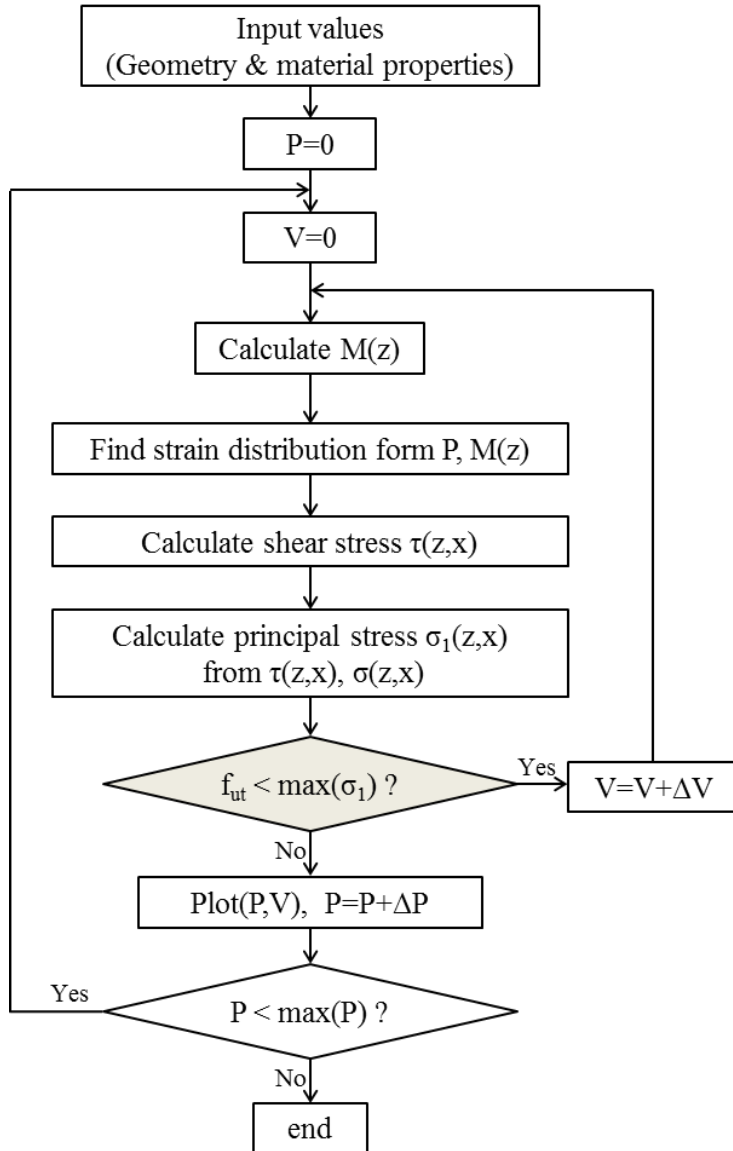
Fig. 4-22 Analysis method for failure mode 3
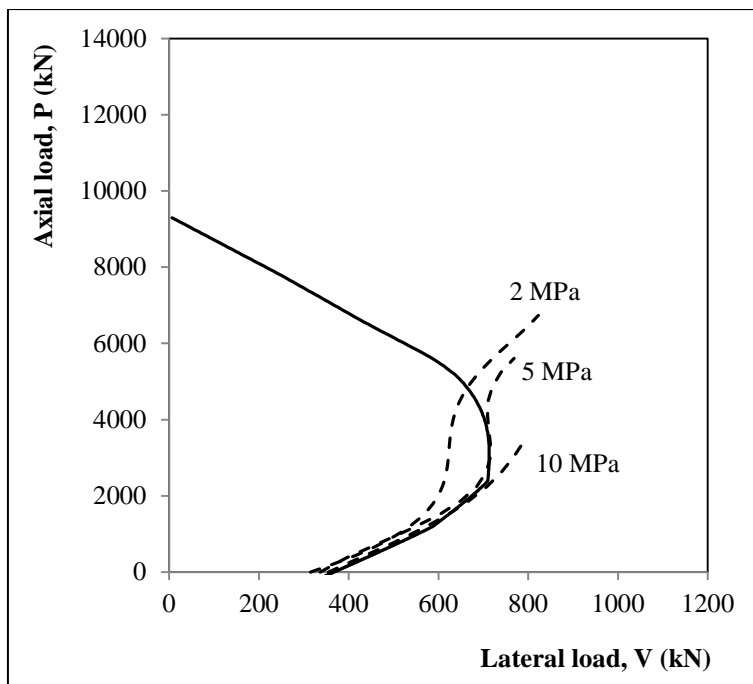
Fig. 4-23 P-V interaction diagram (30mm, mode 3)
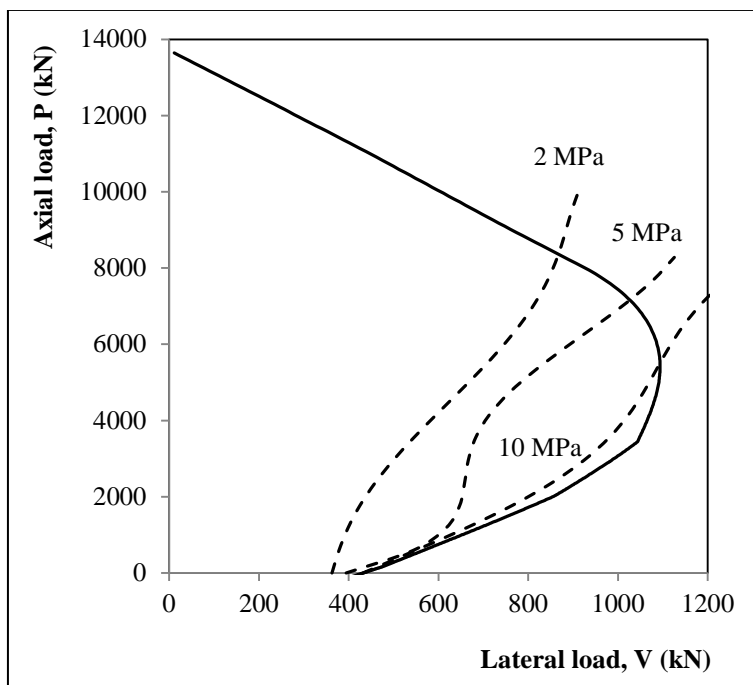
Fig. 4-24 P-V interaction diagram (50mm, mode 3)

4.2.5 Analysis result

Fig. 4-25 shows the final P-V interaction diagram including mode 1,2 and 3 for R-50. The interface shear strength was assumed to be 2MPa. It appeared that for normal axial force region, about less than 6000kN, the column would fail in mode 3. The column is prone to fail in mode 2 for higher axial force region and fail in mode 3 for the highest region.

Fig. 4-25 Final P-V interaction diagram (R-50)

For comparison, P-V interaction diagrams for other sections and a/d ratios are plotted as well through Fig. 4-26 to Fig. 4-29. All the jacket thicknesses were unified to 10% of column section width. The failure mode 2 was excluded because for 10% thickness jacket, failure curve for mode 2 was found out to exist outside of failure curve of mode 1.

The result shows quite clear tendency that the a/d ratio do highly influence on the curve shape of mode 3. The failure curves of which a/d ratios are 2.1, Fig. 4-26 and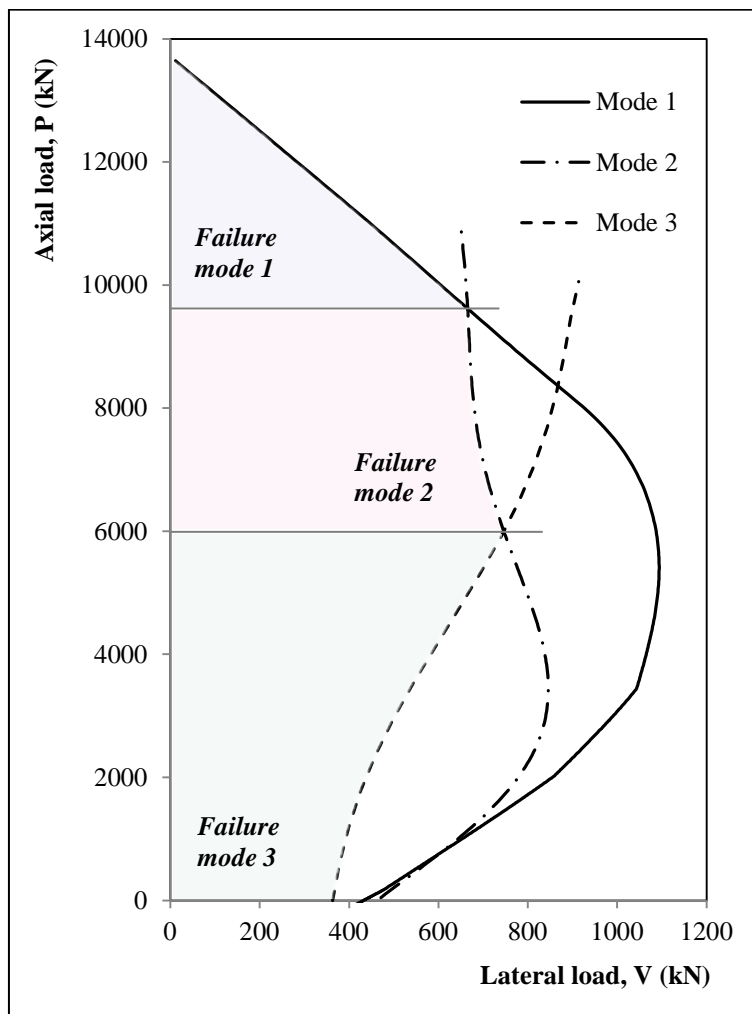 Fig. 4-28, have similar shapes and seem to require interface shear strength of 10MPa to get to be outside of failure curve of mode 1. In contrast, Fig. 4-26 and Fig. 4-28 shows the failure curve whose a/d ratios are 3. It is estimated that they only require interface shear strength of about 5MPa to get out of mode 1 failure curve.

It may be required to add some clamping bars as well as surface roughening treatment to satiyfy the interface strength. The amount of the clamping bars to secure the interface shear strength more than 5MPa can be estimated by the formula $\rho f_{yd} \left(\mu \sin \alpha + \cos \alpha \right)$. The cohesion contribution would be 2MPa as estimated in 4.2.3. Than clamping contribution should be more than 3MPa. Assuming $f_{yd} = 400\text{MPa}$ and $\mu = 1.34$, than the shear reinforcement ratio, ρ is calculated about 0.006. This value is quite large in that for it requires at least two sets of #3 bars per every 100mm for 300mm-width column. Therefore, it would be very uneconomic to secure high interface shear strength using clamping bars.

Instead of bringing up interface shear strength, to increase a tensile strength of jacket would be more economic and also easier to construct. In

order to raise up the tensile strength of UHPC itself is limitative as the amount of steel fiber is limited. Therefore, adding some additional stirrups or meshes inside the jacket would be advisable to secure high tensile strength of jacket and to control post-cracking behavior.
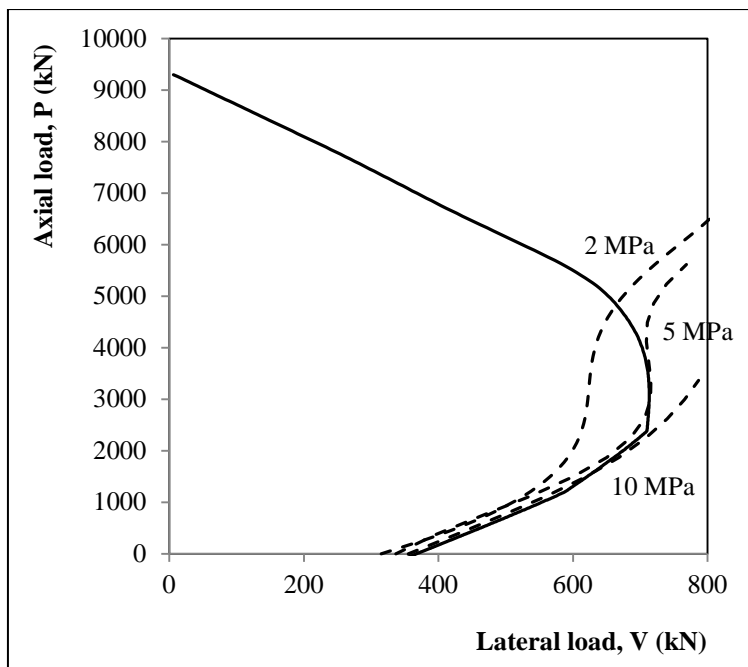
Fig. 4-26 P-V diagram (b=300mm, ρ=2.1)

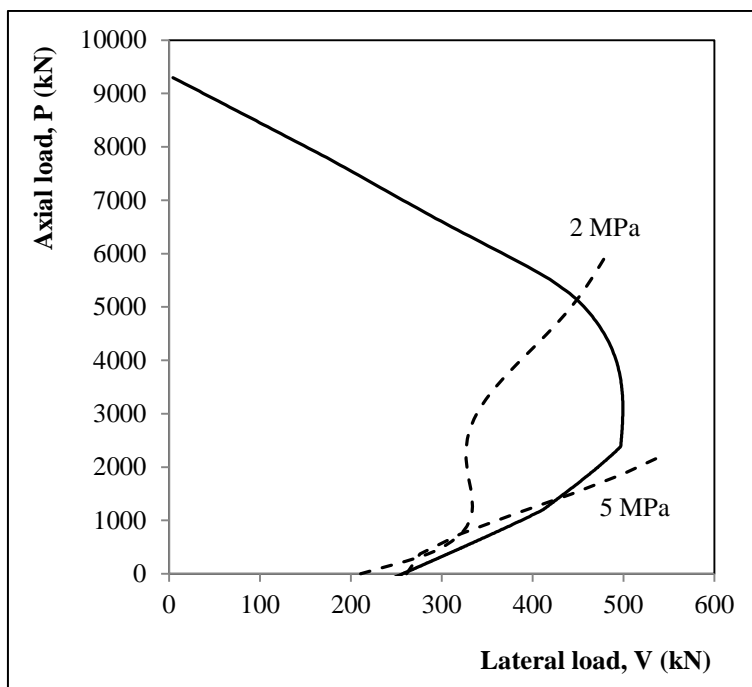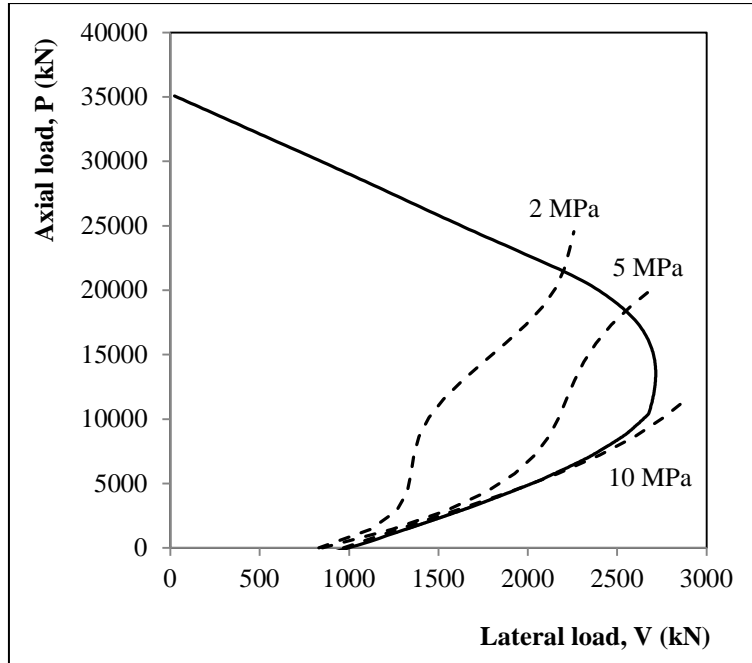**Fig. 4-27 P-V diagram (b=300mm, ρ=3.0)**

Fig. 4-28 P-V diagram (b=600mm, ρ=2.1)

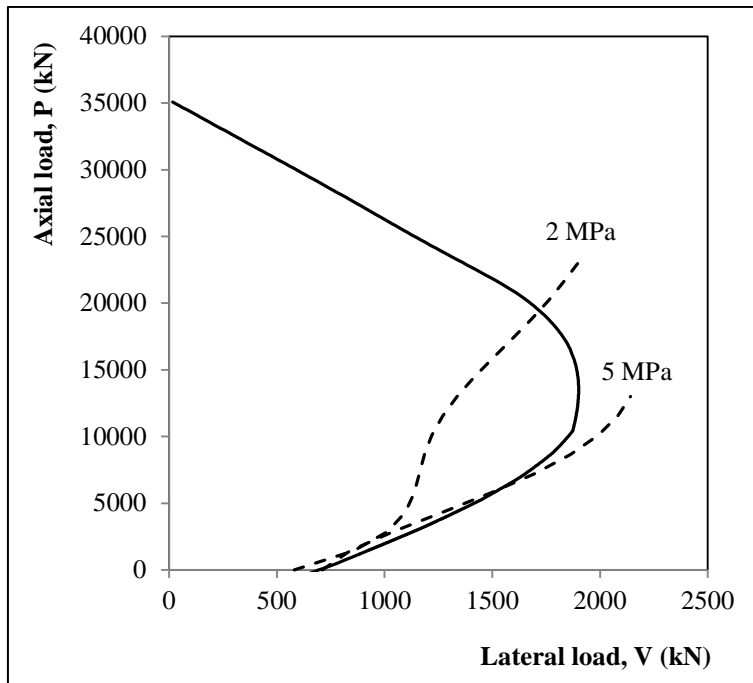**Fig. 4-29 P-V diagram (b=600mm, ρ=3.0)**

Chapter 5. Conclusion

In this study, the lateral load resistance capacity of RC column retrofitted with ultra high performance concrete (UHPC) jacket was estimated through an experiment and theoretical analysis. In order to secure high constructability the jacketing method considered in this study was just a simple jacketing without any measures such as additional longitudinal reinforcements or shear stud between jacket and core. For interface treatment, surface roughnening process using sandblasting was applied.

In chapter 3, the experimental result was analyzed. The experiment was implemented with variables of jacket thickness and stirrup insert. The lateral load capacities of the retrofitted columns have increased about 70~130% depending on jacket thickness. The columns reached their maximum strength when they got the diagonal tension crack in the web of the jacket. The columns went to failure soon after crack occured. Although steel fibers contribute to sustain the crackings from further opening, it is considered insufficient.

In the specimen with additional stirrups inserted inside the jacket, the result shows much higher performance especially in ductility. The stirrups in jacket prevent massive diagonal cracking that other specimens has occurred. This made the retrofitted column sustain the lateral load far beyond the yielding point. However, it is judged that the excessively high ductile behavior was influenced by relatively weak base strength in that the cracks occurred in base stub was found to be too large and these cracks must have absorbed significant amount of energy and reduced stress which otherwise

should have applied to column or jacket.

In chapter 4, possible failure mode for the UHPC jacketed RC column was analyzed with some assumptions. Based on experimental results, failure mode of UHPC jacketed column was classified into three modes: flexural compressive failure, direct shear failure between flange and web of the jacket, diagonal shear failure of web of the jacket. Failure curves for the possible failure modes were plotted in interaction diagram between axial and lateral load. For each mode, failure criteria was set and the failure condition was found by numerical method. The result shows that in normal axial load condition, the retrofitted columns are prone to fail in diagonal tension failure, which accord with experimental result. This is due to the composition of composite section, which has high stiffness outside and low stiffness inside.

In order to avoid premature diagonal tension failure, two additional measures can be taken. First, interface shear strength can be secured by adding clamping reinforcements as well as surface roughening. However, this method requires too much works, as the required interface shear strength is very high. Second, additional stirrups or meshes can be added inside jacket to prevent the jacket from failure by diagonal tension cracks.

This research is expected to be used as a reference for suggesting design method and strength expressions of UHPC jacketing for RC column. Further experimental research would be necessary that has variables of applied axial load or surface treatment in order to verify the failure mode analysis result of this study.

References

ACI committee 318. 2011. American Concrete Institute, Farmington Hills, MI Building Code Requirements for Structural Concrete and Commentary.

An, X., and Maekawa, K. 1998. *Shear Resistance and Ductility of RC Columns after Yield of Main Reinforcement.* Paper presented at the PROCEEDINGS-JAPAN SOCIETY OF CIVIL ENGINEERS.

ASCE/SEI 41-13. 2014. Seismic Evaluation and Retrofit of Existing Buildings, American Society of Civil Engineers.

Beschi, C., Meda, A., and Riva, P. 2009. "High Performance Fiber Reinforced Concrete Jacketing in a Seismic Retrofitting Application". Paper presented at the ATC & SEI conference on Improving the Seismic Performance of Existing Buildings and Other Structures.

Beschi, C., Meda, A., and Riva, P. 2011. "Column and Joint Retrofitting with High Performance Fiber Reinforced Concrete Jacketing". *Journal of Earthquake Engineering, 15*(7), 989-1014.

Chynoweth, G., Stankie, R. R., Allen, W. L., Anderson, R. R., Babcock, W. N., Barlow, P., . . . Constantino, F. J. 1996. "Concrete repair guide". *ACI committee, concrete repair manual, 546*, 287-327.

Committee, A., Institute, A. C., and Standardization, I. O. f. 2008. *Building code requirements for structural concrete (ACI 318-08) and commentary*.

Lampropoulos, A., and Dritsos, S. E. 2011. "Modeling of RC columns strengthened with RC jackets". *Earthquake Engineering & Structural Dynamics, 40*(15), 1689-1705.

Lee, J.-H., and Hong, S.-G. 2015. " Shear Friction Strength based on Limit Analysis for Ultra-High Performance Fiber Reinforced Concrete". *Journal of the Korea Concrete Institute, 27*(3), 296-306.

Lee, J., Nishiyama, M., Kono, S., and Sakashita, M. 2015. "Diagonal Tension Failure of Reinforced and Prestressed Concrete Member". *ACI Structural Journal, 112*(3), 311.

MacGregor, J. G., Wight, J. K., Teng, S., and Irawan, P. 1997. Reinforced concrete: mechanics and design (Vol. 3): Prentice Hall Upper Saddle River, NJ.

Meda, A., Mostosi, S., Rinaldi, Z., and Riva, P. 2016. "Corroded RC columns repair and strengthening with high performance fiber reinforced concrete jacket". *Materials and Structures, 49*(5), 1967-1978.

Meda, A., Plizzari, G., Rinaldi, Z., and Martinola, G. 2009. "Strengthening of R/C Existing Columns with High Performance Fiber Reinforced Concrete Jacket".

Minafò, G. 2015. "A Practical Approach for The Strength Evaluation Of Ro Columns Reinforced with RC Jackets". *Engineering Structures, 85*, 162-169.

Mohamad, M. E., and Ibrahim, I. S. 2015. "Interface Shear Strength of Concrete-to-Concrete Bond with and without Projecting Steel Reinforcement". *Jurnal Teknologi, 75*(1).

Pan, Z., and Li, B. 2012. "Truss-Arch Model for Shear Strength of Shear-Critical Reinforced Concrete Columns". *Journal of Structural Engineering, 139*(4), 548-560.

Santos, P. M., and Júlio, E. 2014. "Interface Shear Transfer on Composite Concrete Members". *ACI Structural Journal, 111*(1), 113-121.

Takiguchi, K. 2001. "Shear Strengthening of Reinforced Concrete Columns Using Ferrocement Jacket". *Structural Journal, 98*(5), 696-704.

Tayeh, B. A., Bakar, B. A., and Johari, M. M. 2013. "Characterization of The Interfacial Bond between Old Concrete Substrate and Ultra High Performance Fiber Concrete Repair Composite". *Materials and Structures, 46*(5), 743-753.

Thermou, G., Pantazopoulou, S., and Elnashai, A. 2007. "Flexural Behavior of Brittle RC Members Rehabilitated with Concrete Jacketing". *Journal of Structural Engineering, 133*(10), 1373-1384.

Vandoros, K. G., and Dritsos, S. E. 2006. "Interface Treatment in Shotcrete Jacketing of Reinforced Concrete Columns to Improve Seismic Performance". *Structural Engineering and Mechanics, 23*(1), 43-61.

Vandoros, K. G., and Dritsos, S. E. 2008. "Concrete Jacket Construction Detail Effectiveness When Strengthening RC Columns". *Construction and Building Materials, 22*(3), 264-276.

초 록

초고성능 콘크리트를 이용한 기둥 보강 연구

구 인 영

서울대학교 건축학과 대학원

UHPC는 초고성능 콘크리트는 압축강도 180MPa 이상, 인장강도 10MPa 이상 발휘할 수 있는 재료로서 구조 보강재로의 연구 및 적용이 활발히 진행되고 있다. 본 연구에서는 UHPC의 가장 큰 장점인 강한 압축력을 효율적으로 이용할 수 있는 기둥보강에 관한 연구를 수행하였다. UHPC를 활용한 기둥 보강은 일반 콘크리트 자켓팅보다 적은 두께로 설계가 가능하고, 타공법에 비해 보강 성능이 뛰어날 것으로 예상되며, 내구성이나 내화성, 내마모성 등에서도 탁월한 성능을 기대할 수 있다.

본 연구는 UHPC 자켓을 이용한 보강방법 중 시공성을 고려하여, 추가적인 휨철근이나 전단 연결재 등을 사용하지 않고 기존 기둥을 순수 UHPC 자켓만을 사용하여 보강했을 때의 보강 성능을 확인하는데 목적을 두었다. 기둥의 내진 보강 시 요구되는 여러 성능 중 횡강도 보강 성능 평가에 주 초점을 두었으며, 이를 위하여 관련 실험과 보강 기둥의 파괴 모드 및 강도에 관한 이론적인 분석을 실시하였다.

자킷 두께에 따른 보강 실험에서는 두께에 따라 횡강도가 우수한 보강 성능을 확인하였다. 띠철근을 추가 배근하지 않은 실험체의 경우에는 자킷의 사인장 균열로 파괴되었으며, 사인장 균열 발생이후에 자킷의 성능이 급격히 감소하는 것을 결과를 보였다. 또한, UHPC 자킷팅이 인접 보나 슬라브에 추가적인 전단력을 가하여, 예상치 못한 파괴가 발생할 수 있으므로, 이에 대한 고려가 필수적이며, 기둥보강시에는 보나 슬라브의 오버레이 공법과 병행하여 사용하는 것이 바람직할 것이다.

파괴 모드 분석에서는 세가지 파괴를 산정하고 그에 따른 파괴곡선을 축력과 횡력에 관한 상관도에 나타내었다. 그 결과, 부재에 횡력이 작용할 경우 강성이 강한 UHPC가 내부 기둥을 감싸고 있는 단면의 특성상 일반적인 RC 합성 단면에 비하여 계면 전단력이 크게 작용하며, 계면 전단 강도가 충분히 크지 않은 경우 기둥이 사인장균열에 의해 파괴될 확률이 높다는 것을 확인하였다. 따라서 UHPC 자킷 적용시 보다 우수한 성능 발휘를 위해서는 자킷 내부에 추가 철근이나 메쉬를 삽입하여 사인장 균열의 발생 및 벌어짐을 제어하는 것이 필요하며 이에 대한 공법 및 성능에 관한 추가 연구가 요구하다.

핵심용어 : 초고성능콘크리트(UHPC), 기둥, 보강

학번 : 2015-21094